Provenance and tectonic setting of Carboniferous–Triassic sandstones from the Karaburun Peninsula, western Turkey: A multi-method approach with implications for the Palaeotethys evolution

Kersten Löwen[a,*], Guido Meinhold[a, b], Talip Güngör[c]

[a] Abteilung Sedimentologie/Umweltgeologie, Geowissenschaftliches Zentrum Göttingen, Universität Göttingen, Goldschmidtstraße 3, 37077 Göttingen, Germany

[b] School of Geography, Geology and the Environment, Keele University, Keele, Staffordshire, ST5 5BG, UK

[c] Department of Geological Engineering, Dokuz Eylül University, Tinaztepe Campus, 35160 Buca-İzmir, Turkey

*e-mail: kersten.loewen@geo.uni-goettingen.de

Tel.: +49 551 399818

Abstract

Carboniferous–Triassic siliciclastic sediments of the Karaburun Peninsula in western Turkey were studied to unravel their provenance and the tectonic setting of depositional basins within the Palaeotethyan realm. A set of complementary techniques including petrography, bulk-rock geochemistry and single-grain analysis of rutile, garnet and chrome spinel were applied to provide a diverse dataset for testing existing palaeotectonic models using both, established and recently published diagrams. We show that tectonic discrimination diagrams of siliciclastic sediments based on major and trace element whole-rock geochemical data do yield ambiguous results and are only partly in accordance with regional geological events. Chondrite-normalised REE patterns of Upper Palaeozoic samples are characterised by enrichment of LREE and a flat trend towards HREE. The degree of fractionation allows for discrimination between sandstones of Karaburun (La_N/Yb_N = 8.00–14.79) and adjacent Greek islands of Chios (5.82–9.23) and Inousses (7.40–9.95). Petrographic observations and compositional data from single-grain analysis indicate significant supply from low- to medium-grade metamorphic rocks of generally felsic character and minor input of (ultra)mafic detritus. Detrital chrome spinels in the Lower Triassic Gerence Formation are different in composition and shape compared to chrome spinels in Carboniferous–Permian sandstones. They were derived from a very proximal source and exhibit variable, but generally high Cr- and Mg-numbers, consistent with chrome spinels from podiform chromitites that have been formed in an intra-oceanic back-arc setting above a supra-subduction zone. We conclude that most of the Carboniferous–Triassic successions were deposited along the southern active margin of Eurasia in a continental-arc environment during the time period when Palaeotethys diminished in size and finally vanished. Large volumes of detritus were probably derived from rock units located in the present-day Balkan region and the Sakarya Zone, or equivalent successions that are not present anymore.

Keywords: petrography; geochemistry; mineral chemistry; Palaeotethys; Karaburun Peninsula; Turkey

1. Introduction

The Eastern Mediterranean region is an integral part of the Alpine–Himalayan system and is made up of several continental fragments which document a complex geodynamic history. The major tectonic units and suture zones in western Turkey are, from N to S, the İstanbul Zone, the Sakarya Zone, the İzmir–Ankara Zone, the Menderes Massif, the Lycian nappes, and the Taurides (Fig. 1a).

The Late Palaeozoic to Early Mesozoic period in the Eastern Mediterranean region was strongly influenced by the evolution of the Tethyan oceans. The Palaeotethys is considered as an oceanic domain that originated in early to mid-Palaeozoic time separating Gondwana and its detached continental fragments from Eurasia (e.g., Şengör et al., 1984; Stampfli and Borel, 2002; Stampfli et al., 2013). Northward drift of the Gondwana-derived Cimmerian continents mostly during the Permian–Triassic and an evolving Neotethys to the south led to subduction of the Palaeotethys, but the timing of final closure remains controversial (e.g., Şengör et al., 1984; Stampfli and Borel, 2002; Stampfli et al., 2013).

Chios Island (Greece) and Karaburun Peninisula (W Turkey) are regarded as key areas for understanding the closure history of the Palaeotethys as they exhibit virtually unmetamorphosed Palaeozoic to Mesozoic sedimentary rocks (e.g., Besenecker et al., 1968; Erdoğan et al., 1990; Kozur, 1998; Robertson and Pickett, 2000; Zanchi et al., 2003; Meinhold et al., 2007, 2008a, b; Robertson and Ustaömer, 2009a). Their role within the Palaeotethyan realm has been interpreted in different ways and both the northern margin of Gondwana (e.g., Robertson and Picket, 2000; Robertson and Ustaömer, 2009a; Akal et al., 2011) and the southern Eurasian margin (e.g., Stampfli, 2000; Stampfli et al., 2003; Moix et al., 2008) have been proposed as palaeopositions for the Late Palaeozoic. This uncertainty is mainly due to the lack of reliable data for testing the various palaeotectonic models. Few available provenance data include detrital zircon U–Pb ages from both localities as well as bulk-rock geochemistry and compositional data of rutile and chrome spinel from Chios Island that suggest deposition along the southern Eurasian margin in the Late Palaeozoic (Meinhold

et al., 2007, 2008a, b; Löwen et al., 2017). Alternatively, other authors propose a northern Gondwana affinity (e.g., Robertson and Pickett, 2000; Akal et al., 2011). They refer to similar stratigraphic characteristics (continuous Early Triassic to Late Cretaceous carbonate deposition) of the study area and the Anatolide–Tauride platform while important features of the Pontides (Liassic unconformity and Triassic high-pressure metamorphism) related to the evolution of the Eurasian continent are missing.

The aim of this study is to shed light on the provenance and the depositional tectonic setting of sediments from the Karaburun Peninsula. The reconstruction of source areas will allow us to test current palaeotectonic models and either support or exclude some of those. We present and discuss data from a multi-method approach including data from thin section petrography, whole-rock geochemistry, and single-grain geochemistry of detrital rutile, garnet and Cr-spinel (this study), supplemented by detrital zircon U–Pb ages (Löwen et al., 2017). Samples were taken from siliciclastic sections of Upper Palaeozoic (i.e., Küçükbahçe, Dikendağı and Alandere formations) to Upper Triassic (i.e., İdecik unit, Gerence, and Güvercinlik formations) successions to monitor provenance changes during this important time period when Palaeotethys diminished in size and finally vanished.

2. Geological setting

The Karaburun Peninsula is located in the central, westernmost part of Turkey adjacent to the Aegean Sea (Fig. 1a). It is part of the İzmir–Ankara Zone, a suture zone separating continental fragments of Eurasian affinity (e.g., units within the Sakarya Zone to the north) from fragments of Gondwana affinity (e.g., Menderes Massif to the south) (e.g., Okay and Tüysüz, 1999; Stampfli, 2000; Moix et al., 2008). Despite considerable effort – several studies and mappings were carried out in the area during the past >100 years (e.g., Philippson, 1911; Kalafatçıoğlu, 1961; Erdoğan et al., 1990; Robertson and Pickett, 2000; Stampfli et al., 2003; Çakmakoğlu and Bilgin, 2006; Robertson and Ustaömer, 2009a) – the exact tectono-stratigraphic situation and timing of sediment deposition, especially for the Palaeozoic succession, are not fully understood. By the current state of knowledge large

parts of the northwestern Karaburun Peninsula are made up of two main siliciclastic units, the Küçükbahçe and Dikendağı formations. The structurally lower Küçükbahçe Formation is mainly composed of alternating low-grade metamorphosed (turbiditic) sandstones and shales, without any blocks / olistoliths. These sediments are intensely folded and sheared with pronounced schistosity. The upper siliciclastic part is assigned to the Dikendağı Formation, firstly described by Çakmakoğlu and Bilgin (2006). Robertson and Ustaömer (2009a) refer to it as Karaburun mélange. This succession comprises blocks of black chert and pelagic limestones, ranging in age from Silurian to Carboniferous, and poorly dated volcanic rocks embedded in a highly deformed siliciclastic matrix. In the northern outcrop area of the Dikendağı Formation isolated blocks of black chert are rare. Further south large blocks of limestone and folded chert are highly abundant. The blocks have been dated as Silurian to Carboniferous (black chert) and Silurian to Devonian (limestones) by biostratigraphic data (Kozur, 1995, 1997, 1998). Main distinctive features compared to the Küçükbahçe Formation are the occurrence of blocks / olistoliths and a very slight schistosity indicative for a lower metamorphic grade. The contact between the Küçükbahçe and Dikendağı formations is tectonic. Two granitoid intrusions crop out in the northern part of the Karaburun Peninsula whose age has been constrained to Early Triassic by a biotite Rb–Sr isochron age of 239.9 ± 2.4 Ma (Ercan et al., 2000) and zircon U–Pb ages of 244.4 ± 1.5 Ma (Ustaömer et al., 2016) and 247.1 ± 2.0 Ma, respectively (Akal et al., 2011). Local exposures of the Alandere Formation at the southern coast area of Gerence Bay (Fig. 1b) were interpreted as structurally highest part within the Karaburun mélange by Robertson and Pickett (2000). The Alandere Formation is predominantly composed of fossil-rich, shallow-water limestones and contains sandstones, conglomerates, shales and chert. The age is well constrained by biostratigraphic data to Carboniferous (Serpukhovian–Bashkirian) (Erdoğan et al., 1990, 2000). This whole Palaeozoic succession (i.e., Küçükbahçe, Dikendağı and Alandere formations) was previously also interpreted as Ordovician–Carboniferous sedimentary sequence, separated by gradational contacts (Çakmakoğlu and Bilgin, 2006). In contrast, a recent study on detrital zircon ages from these sediments indicates sediment

deposition of the Küçükbahçe and Dikendağı formations probably began in the mid-Carboniferous and continued to at least Pennsylvanian–Cisuralian (Löwen et al., 2017). In the light of these findings a revised stratigraphic section was presented, interpreting this sequence as a pile of units deposited in Carboniferous–Early Permian times, separated by tectonic rather than gradational contacts (Fig. 2).

According to Robertson and Pickett (2000) and Robertson and Ustaömer (2009a), the Late Palaeozoic Karaburun mélange is unconformably overlain by a thick sequence dominated by Mesozoic platform carbonates, that make up large parts of the eastern and southern area of Karaburun Peninsula. This succession is of Early Triassic to Late Cretaceous (Campanian–Maastrichtian) age and is subdivided into several units, including the Gerence Formation, İdecik unit, Camiboğazı Formation and Güvercinlik Formation (Çakmakoğlu and Bilgin, 2006). The Gerence Formation unconformably overlies the Karaburun mélange. At its base, it consists of a siliciclastic part dominated by conglomerates with reworked material of underlying formations and intervals of sandstones developing into more carbonate-rich conglomerates at the top. An Early Triassic age has been assigned to this formation by abundant fossils (ammonites, conodonts, foraminifera). This unit is followed by thick-bedded, massive limestones of the Camiboğazı Formation, determined to be of Middle–Late Triassic (Ladinian–Carnian) age (e.g., Brinkmann et al., 1972; Erdoğan et al., 1990, 2000). The gradationally overlying Güvercinlik Formation is a detritic succession of highly mature, red sandstones, conglomerates and fossiliferous (Megalodon bivalves, algae, gastropods) oolitic and dolomitic limestones of Late Triassic age (Stampfli et al., 2003; Çakmakoğlu and Bilgin, 2006). Small exposures in the central part of northern Karaburun Peninsula are assigned to the İdecik unit that is tectonically thrust in between the Karaburun mélange and the Gerence Formation. Volcanoclastic rocks, basic lavas, tuffaceous material, limestones and radiolarites of Ladninian–Carnian age are the main constituents of this unit (Çakmakoğlu and Bilgin, 2006).

3. Methodology

A total of eighteen siliciclastic sedimentary rocks of Carboniferous to Late Triassic age were collected from the Karaburun Peninsula for petrographic and whole-rock geochemical analysis as well as mineral chemistry of garnet, rutile and chrome spinel. Sample localities are shown in Fig. 1b, and a list of samples including GPS coordinates and information on conducted analyses is given in Table 1. All steps of preparation and geochemical analyses were performed at the Geoscience Center Göttingen (Department of Sedimentology and Environmental Geology and Department of Geochemistry). Samples were cut with a rock saw to have rock slices for thin section preparation. The remaining material was crushed by a jaw crusher and disc mill. Part of the material was grinded to <63 µm by an agate ball mill for whole-rock geochemical analysis. The remaining material was wet-sieved using a mechanical shaker to separate different grain-size fractions. The 63–250 µm fraction was decarbonated with acetic acid (5%) and heavy minerals were extracted in separation funnels using sodium polytungstate ($Na_6[H_2W_{12}O_{40}]$, ρ = 2.85 g/cm^3).

Thin sections were analysed using a petrographic microscope with an attached point counting stage. At least 300 points were counted for each sample according to the Gazzi-Dickinson method (e.g., Ingersoll et al., 1984). Recorded components include mono- and polycrystalline quartz (Q_m, Q_P), plagioclase (P), alkali feldspar (K-fsp) and lithic fragments (L). Matrix and cement were not counted but estimated using standard charts for visual percentage estimation.

Whole-rock geochemical analyses were carried out using a PANalytical AXIOS Advanced sequential X-ray spectrometer. Fused glass discs were produced by adding Spectromelt® and LiF to the sample powder and melting in platinum crucibles. Loss on ignition (LOI) was determined gravimetrically by stepwise heating to 1000 °C.

Solution inductively coupled plasma mass spectrometry (ICP–MS) for trace element geochemistry was applied to eight samples (at least one from each formation). Sample powder (~50 mg per sample) was dissolved by PicoTrace® acid digestion system. Analytical procedures were started by pre-reaction with 2 ml HNO_3 at 50 °C overnight. After cooling to room temperature samples were treated with 3 ml HF and 3 ml $HClO_4$ and heated to 150 °C

for 8 hours during the first pressure phase. For evaporation the digestion vessels were heated to 180 °C for 16 hours. After cooling 10 ml H_2O (double de-ionised), 2 ml HNO_3 and 0.5 ml HCl were added to the samples for the final pressure phase and re-heated to 150 °C for 4 hours. Internal standard (100 µl) for ICP–MS analysis was added to the solution after final cooling. Trace element analysis was performed on a ThermoElectron VG PlasmaQuad 2 quadrupole ICP–MS. All analytical data for main and trace element geochemistry are given in the accompanying Supplementary data (see Appendix A).

Mineral chemical analyses of garnet, rutile and chrome spinel were applied to a selection of samples, depending on the presence of the specific minerals, covering formations from mid-Carboniferous to Late Triassic age. Mineral grains were extracted from the 63–250 µm fraction and randomly selected by handpicking under a stereomicroscope and placed on synthetic mounts using an epoxy resin composed of a mixture of Araldite® and hardener (5:1). Prior to analysis, the polished grain mounts were carbon-coated to ensure conductivity. Geochemical measurements were carried out with a JEOL JXA 8900 RL electron microprobe analyzer (EMPA) equipped with five wavelength dispersive spectrometers. The analytical data, measurement parameters and spectrometer configurations are given in the accompanying Supplementary data (see Appendix A).

4. Results

4.1. Petrography

Petrographic analysis included identification of mineral phases and lithic fragments, counting of grains for QFL classification, and estimation of textural maturity based on grain sorting and degree of rounding. Mineralogy and QFL compositions are given in Table 2. Classification of siliciclastic sedimentary rocks was done using the relative proportions of quartz, feldspar and lithic fragments (after McBride, 1963), and additionally based on their chemical composition according to their logarithmic ratios of SiO_2/Al_2O_3 vs. Fe_2O_3/K_2O (Herron, 1988) (Fig. 3). An overview of results from petrographic analysis is given in Fig. 4. With few exceptions, the analysed sandstones are made up of at least 75% quartz and variable amounts of feldspar

(mainly plagioclase) and lithic fragments. Feldspar content is generally between 5–10% (max. 30%), whereas the amount of rock fragments is highly variable (up to 40%) and usually higher in the Triassic samples (e.g., Gerence Formation and İdecik unit).

The only sample from the Serpukhovian–Bashkirian Alandere Formation (KAR22) is a subarkosic rock, representative of the lower clastic part (Fig. 1b). The sediment is mainly composed of quartz and plagioclase with minor K-feldspar. Lithic fragments are of primarily volcanic and rare sedimentary origin and carbonate clasts occur sporadically (Fig. 6a). Non-opaque accessory minerals include zircon, tourmaline, garnet, rutile and chrome spinel. Textural immaturity is indicated by poor sorting and (sub)angular grain shape.

Five samples were collected from the northern, southern and central part of the Küçükbahçe Formation, one of the main siliciclastic units of the Karaburun Peninsula (Fig. 1b). The fine-medium grained sandstones reveal low textural maturity (moderately to well sorted, angular to subangular grains) and were classified as (sub)litharenites and (sub)arkosic rocks. Their texture is often characterised by preferential alignment of slighlty deformed grains and lithic fragments. These clasts occur in low to moderate amounts (4–15%) and were almost entirely derived from sedimentary sources (clastic sedimentary and chert fragments), the exception being one sample (KAR27) with predominant volcanic fragments. Feldspar is equally abundant (6–11%) with plagioclase as the dominant phase. The assemblage of accessory heavy minerals contains mostly tourmaline, zircon and rutile but garnet and chrome spinel exclusively occur in two different samples (KAR9 and KAR27).

Six sandstones were collected from the northern and southern part of the Dikendağı Formation, the second main Palaeozoic siliciclastic unit of the Karaburun Peninsula (Fig. 1b). In contrast to the comparatively homogeneous Küçükbahçe Formation these samples are characterised by higher compositional variability and generally low textural maturity. Two fine- to medium-grained sediments, a sublitharenite (KAR5) and a lithic subarkose (KAR 6) from the southern part of the formation exhibit moderate amounts of lithic fragments (10–13%) from metapelitic and mafic volcanic rocks (Fig. 6b). The texture is dominated by poorly- (KAR5) to well-sorted (KAR6) grains of (sub)angular shape (Fig. 5b). Three fine-grained

subarkosic rocks (KAR14, KAR15, KAR23) from the northern part, however, are slightly more mature and contain negligible amounts of lithic sedimentary fragments only (1–4%). Another sample (KAR7), classified as lithic arenite was taken from the southwestern coastal part of the study area. Its particular textural and compositional properties are characterised by considerably coarse and highly variable grain size and angular components. A striking feature is the high abundance of lithic volcanic rock fragments and large, subhedral plagioclase (mainly albite) and K-feldspar crystals (up to 2 mm) (Figs. 5d, 6c). The heavy mineral assemblage of these rocks is dominated by tourmaline, zircon, rutile and titanite but garnet and chrome spinel are absent.

From the İdecik unit, two samples were collected in close distance to the Dikendağı Formation near Gerence Bay in the western part of the Karaburun Peninsula (Fig. 1b). The sediments are classified as fine- to medium-grained sublitharenites (KAR3) and litharenites (KAR4), respectively. Petrographic features are very similar and their general texture is characterised by poorly-sorted subangular to subrounded grains (Fig. 5e). Quartz is the dominant phase and altered plagioclase and K-feldspar are present in small amounts. Lithic fragments are comparatively abundant and appear as either volcanic or (meta)sedimentary lithoclasts (Fig. 6f).

Two samples were collected from the Lower Triassic Gerence Formation at the west coast of the Karaburun Peninsula at Gerence Bay (Fig. 1b). The first one (KAR1) is a fine- to medium-grained, carbonate-bearing (feldspathic) litharenite with poorly-sorted, subangular grains. Quartz and feldspar (mainly plagioclase) are the dominant phases and few grains show myrmekitic textures (Fig. 5f). Lithic fragments, mainly derived from felsic volcanic rocks are highly abundant (40%) and sedimentary lithoclasts including chert are present but of subordinate importance (Fig. 6g). Non-opaque accessory phases include zircon, apatite, tourmaline, pyroxene, garnet and chrome spinel. In contrast, sample KAR2 is a very fine-grained, mica-rich lithic subarkose with comparatively high textural maturity (Fig. 3a). Its quartz content is considerably higher, whereas lithic fragments are less common. Accessory phases include zircon, amphibole, chloritoid and rutile.

Two samples (KAR20A and KAR20B) of the Güvercinlik Formation were collected from an outcrop at the eastern coast of the Karaburun Peninsula, ca. 4 km north of Balıklıova (Fig. 1b). Both sediments are (highly) mature, medium-grained sublitharenitic rocks. Quartz is by far the most abundant phase and rock fragments are scarce and of sedimentary origin. These are often altered, highly deformed and occupy intergranular spaces (Fig. 6h). Moreover, sample KAR20A contains small amounts of sparitic to micritic carbonate lithoclasts. Non-opaque accessory phases include zircon, garnet, tourmaline, rutile, amphibole (only KAR20A) and orthopyroxene (only KAR20A).

4.2. Whole-rock geochemistry

Whole-rock geochemical data of samples from the Karaburun Peninsula are shown in Fig. 7. Geochemical composition of sediments from the Küçükbahçe and Alandere formations is very homogeneous with respect to major elements. Samples are characterised by moderate SiO_2 (74–77 wt.%) and Al_2O_3 contents (10–12 wt.%), low CaO (<0.75 wt.%), Na_2O (1.9–2.5 wt.%), K_2O (1.3–1.9 wt.%) and Fe_2O_3 contents (3.8–4.9 wt.%). In contrast, samples from the Dikendağı Formation are highly variable in major element compositions with low to high SiO_2 (64–83 wt.%), moderate to high Al_2O_3 (8–17 wt.%) and Na_2O contents (0.7–5.5 wt.%). Combination of high Al_2O_3 and Na_2O concentrations document abundant albite components for sample KAR7, as confirmed by petrographic observations. Geochemistry of samples from the İdecik unit is comparable with the Küçükbahçe Formation with the exception of slightly lower Fe_2O_3 (2.9–3.9 wt.%) and comparatively high TiO_2 contents (0.8 wt.%). Two sediments of the Gerence Formation have the lowest overall SiO_2 content (62–69 wt.%; except of KAR7), moderate to high Al_2O_3 content (10–15 wt.%) and high Fe_2O_3 content (~5 wt.%). Samples from the Güvercinlik Formation are highly mature and characterised by very high SiO_2 contents (>90 wt.%) and only traces of Na_2O (<0.02 wt.%). Low values of CaO and LOI for all sandstones – except of sample KAR1 (CaO ~ 8 wt.%) – indicate an almost complete absence of carbonate-bearing phases.

Chondrite-normalised rare earth element (REE) patterns of selected sandstone samples from the Karaburun Peninsula (this study) and reference data from time equivalent deposits of the neighboring islands of Chios and Inousses (Meinhold et al., 2007) are shown in Fig. 8. Triassic samples can be easily discriminated on the basis of their REE composition. Sample KAR1 from the Gerence Formation has a unique REE composition with almost no fractionation between LREE and HREE. In contrast, all other samples, including the samples of Chios and Inousses, have comparable REE patterns with only little variation. They show notably strong enrichment of LREE, followed by a decrease towards Sm, a negative Eu anomaly and flattening out towards the HREE. Due to its high amount of plagioclase sample KAR7 (Dikendağı Formation) has a positive Eu anomaly. Although these samples show similar behavior, the ratios of La_N/Yb_N as a measure for the degree of fractionation between LREE and HREE turned out to be a good indicator for discrimination of the different sedimentary successions. For the Upper Palaeozoic sandstones from the Karaburun Peninsula the fractionation is more pronounced (La_N/Yb_N = 8.00–14.79) compared to samples from Chios (5.82–9.23) and Inousses (7.40–9.95). Sample KAR20B from the Upper Triassic Güvercinlik Formation has a comparable pattern, but the REE concentrations are considerably lower.

Selected trace element concentrations for samples from the Karaburun Peninsula have been normalised to upper continental crust (UCC) and are shown in multielement diagrams (Fig. 9). These include the large-ion lithophile elements (LILE; e.g., Rb, Ba, Sr) and high-field-strength elements (HFSE; e.g., Zr, Hf, Nb, Ta). Concentration of incompatible and easily mobilised LILE is generally controlled by the presence/absence of feldspar, and LILE are generally enriched in UCC compared to the mantle. The (highly) incompatible HFSE, however, are considered to be relatively immobile and therefore can provide additional information on sedimentary provenance (Taylor and McLennan, 1985). During magmatic differentiation processes the HFSE are preferentially partitioned into the melt phase resulting in enrichment in felsic rather than mafic rocks (Bauluz et al., 2000). The similar behavior of Zr and Hf in our samples, revealed by a strong positive linear correlation (r = 0.96) indicates

their concentrations are coupled to the mineral zircon, whereas rutile and monazite are major carriers of HFSE as well (Deer et al., 1992). Patterns of UCC-normalised trace element concentrations from the Upper Palaeozoic Küçükbahçe, Dikendağı and Alandere formations and the Ladinian–Carnian İdecik unit are similar with only little variation (Fig. 9a, b, c, e). Their trace element concentrations are slightly below or at UCC level, with few exceptions. Pronounced negative anomalies exist especially for Sr, but also for Ba and K, probably attributed to the general low occurrence of feldspar. HFSE usually exhibit slight positive anomalies suggesting rather prevailing felsic than mafic source rocks. Sediments from the Güvercinlik Formation are highly depleted in all trace elements (except Yb) and define the lower limit of the overall pattern (Fig. 9f). Elevated values of Hf, Zr, Sm, and Yb in one of those samples (KAR20A) are indicative for an enrichment of heavy minerals, especially garnet. Mineralogical compositions of samples from the Gerence Formation are significantly different which is well reflected in their multielement patterns (Fig. 9d). One sample (KAR2) is similar in trace element composition to the above-mentioned samples whereas sample KAR1 is characterised by lower concentrations throughout the whole pattern, positive anomalies of Ba, Sr and P and slight depletion of HFSE.

A compilation of diagrams for the discrimination between felsic and mafic sources and identification of mafic components is shown in Fig. 10. Elemental ratios of Cr/V and Y/Ni were used as proxies for (ultra)mafic components, i.e., in particular chrome spinel which is a key mineral in mafic and ultramafic rocks. The Y/Ni ratio is a monitor for the concentration of ferromagnesian elements (Ni) in relation to a proxy for the HREE (Y), generally enriched in zircon or garnet (McLennan et al., 1993). Thus, ultramafic (ophiolitic) sources tend to have high Cr/V but low Y/Ni ratios. Samples from the Karaburun Peninsula (black symbols) primarily plot in the lower left area of the diagram, except of two samples with high (>3) Y/Ni ratios (Fig. 10a). Although high Cr/V ratios (1.6–2.2) and low Y/Ni ratios (0.3–0.5) indicate ultramafic components in five samples from the Gerence (KAR1), Alandere (KAR22), Küçükbahçe (KAR27) and Dikendağı (KAR6, KAR15) formations, chrome spinel was only spotted in thin sections and heavy mineral concentrates of sample KAR1, KAR22 and

KAR27. Additionally, Garver et al. (1996) showed that high concentrations of Cr (>150 ppm) and Ni (>100 ppm) combined with Cr/Ni ratios of 1.3–1.5 in sandstones are indicative of ultramafic rocks in the source region as well. Although, total concentrations of Ni and Cr in our samples are low for Ni (3–57 ppm) and variable for Cr (14–240 ppm) and neither samples from the Karaburun Peninsula nor reference samples from the islands of Inousses and Chios meet both criteria, there is evidence of chrome spinel in several of these sediments (Fig. 10b, c, f). The ternary V–Ni–Th×10 and bivariate Th/Sc vs. Cr/Th plots use elements and/or elemental ratios that are sensitive to (ultra)mafic and felsic components, respectively (Fig. 10d, e). High Cr/Th values typify input of mafic character, whereas high Th/Sc values are indicative for detritus derived from felsic rocks (e.g., Hofmann et al., 2003). The signature of our samples in both diagrams suggests rocks of felsic lithology as primary source with variable but minor contribution of mafic detritus. Samples from the Dikendağı Formation are seemingly closer to the felsic composition and a set of samples including KAR1, KAR22 and KAR27 (Gerence, Alandere and Küçükbahçe formations) received notably amounts of mafic components.

4.3. Geochemistry and tectonic settings

Whole-rock geochemical data of sedimentary rocks can provide information for the interpretation of the tectonic setting of depositional basins. Conventional diagrams of Bhatia (1983), Roser and Korsch (1986) or Bhatia and Crook (1986) have been used for a long time to discriminate active and passive continental margin settings, but recent re-evaluations by Verma and Armstrong-Altrin (2013, 2016) contested the efficiency of the existing plots. Verma and Armstrong-Altrin (2013, 2016) used statistical tools and proposed new multidimensional diagrams based on $\log_e$-ratio transformation of major and combined major and trace elements and linear discriminant analysis. These new plots were used in this study in combination with the conventional approach of Roser and Korsch (1986) to decipher the tectonic setting from sedimentary rock geochemistry (Fig. 11). Discriminant functions were calculated using revised equations published in the corrigendum to Verma and Armstrong-

Altrin (2016) (Fig. 11c, d). At first sight the diagrams predict consistent tectonic settings for a small number of samples only, but yield contradictory results for many samples as well. The geochemical signal of the Güvercinlik Formation unambiguously indicates a passive margin setting. Even though samples from the İdecik unit are not equally well defined, a passive margin setting seems most likely as well. Data of the Gerence Formation are of ambiguous character with slight affinities to an active margin setting. However, there are limitations for the discrimination of active and passive tectonic settings, relying solely based on geochemical data. This becomes obvious with respect to the Upper Palaeozoic sediments of the Küçükbahçe and Dikendağı formations. On the one hand, multidimensional diagrams based on major elements clearly indicate an active margin setting (Fig. 11c) and, considering trace elements as well, a passive margin setting on the other hand (Fig. 11d) whereas mixed signals are inferred from additional diagrams (Fig. 11a, b).

4.4. Mineral chemistry

Geochemical single-grain analysis of detrital heavy minerals is a complementary technique and frequently conducted in sedimentary provenance studies (Mange and Morton, 2007, and references therein). Garnet, rutile and chrome spinel, amongst others, are very useful accessory minerals for deciphering source rock lithologies.

Garnet is a very common heavy mineral that occurs in a wide range of metamorphic and also igneous rocks and is relatively stable during sedimentary transport and burial diagenetic conditions (e.g., Wright, 1938; Morton, 1985; Deer et al., 1992). Its comparatively wide range of major and trace element composition is primarily controlled by host rock composition and reflects changes in pressure and temperature conditions during mineral growth as well. Therefore, mineral chemistry of detrital garnet is widely used as a provenance indicator in studies of sedimentary rocks (e.g., Mange and Morton, 2007; Krippner et al., 2014, 2015, 2016, and references therein).

Rutile is the most common TiO_2 polymorph, mainly formed during medium- to high-grade metamorphic processes; thus eclogites, granulites and high-grade metasediments are the

primary host rocks (e.g., Meinhold, 2010, and references therein). Due to its high chemical and physical resistance during sedimentary processes rutile is widespread in modern and ancient sedimentary rocks, preserving information on source rock lithology. For discrimination of mafic and felsic sources, based on the Cr–Nb system, the most recent criterion proposed by Triebold et al. (2012) was used:

$$x = 5 \times (Nb_{ppm} - 500) - Cr_{ppm}$$

with negative values representing rutiles from mafic rocks and positive values representing rutiles from felsic rocks. Grains with Nb and Cr concentrations below the detection limit were excluded from the calculation.

If possible (i.e., Zr concentration > detection limit) formation temperatures were calculated using the Zr-in-rutile thermometer of Tomkins et al. (2007):

$$T(°C) = \frac{83.9 + 0.410 \times P}{0.1428 - R \times \ln Zr_{ppm}} - 273$$

in which R is the gas constant (0.0083144 kJ/K) and P = 10 kbar (default setting, as no pressure information is available for the detrital rutile grains).

Chrome spinel is a very stable, accessory mineral associated with mafic and ultramafic igneous rocks and is widely used as provenance indicator in studies of sedimentary rocks (e.g., Poper and Faupl, 1988; Cookenboo et al., 1997; Lužar-Oberiter et al., 2009; Caracciolo et al., 2015). Its chemical composition is controlled by several factors, as the behavior of the main components Cr, Mg and Al is different during fractional crystallization or partial melting. Thus, their ratios expressed as Cr-number (Cr#) = Cr / (Al + Cr) and Mg-number (Mg#) = Mg / (Mg + Fe^{2+}) are sensitive to different physicochemical conditions and reveal petrogenetic signatures. Furthermore, the geodynamic setting of source rocks can be deduced from concentrations of Al_2O_3 and TiO_2 in chrome spinel as these elements are linked to magma type and composition (e.g., Cookenboo et al., 1997; Kamenetsky et al., 2001).

4.4.1. Garnet

A total of 156 single grains of detrital garnet were analysed from three samples of the Serpukhovian–Bashkirian Alandere Formation, the Lower Triassic Gerence Formation, and the Upper Triassic Güvercinlik Formation. Compositional data are presented using the triangular diagram for garnet discrimination after Mange and Morton (2007) (Fig. 12). Garnets from the three formations predominantly scatter in the lower left corner of the diagram but, nonetheless, show distinct characteristics. The most diverse garnet population is present in the Güvercinlik Formation with dominant input of type Bi (intermediate to felsic igneous rocks – 48%) and Bii (amphibolite-facies metasediments – 29%) garnet, but small amounts of type Ci (high-grade meta mafic rocks – 14%) and A (granulite-facies metasediments – 9%) grains as well (Fig. 12a). In contrast, the Gerence Formation exhibits considerably higher amounts of Bii (56%) but lower percentage of Bi type (30%) grains with negligible amounts of garnet from high-grade metamafic igneous and granulite-facies metasedimentary rocks (Fig. 12b). Compositional data of garnets from the Alandere Formation are very homogenous and suggest mainly intermediate to felsic igneous rocks (74%) as host lithologies with only minor input of Bii and A type garnets (Fig. 12c).

4.4.2. Rutile

Results for source rock classification from 358 single EMPA measurements of rutiles from eight sandstone samples are shown in Fig. 13. For most of our samples the data indicate a mixture of mafic and felsic sources with a majority of rutiles being derived from felsic rocks (44–78%) (Fig. 13a). However, rutiles from the Küçükbahçe Formation and İdecik unit (KAR4) indicate significant supply from mafic source rocks (49–56%).

Results of Zr-in-rutile thermometry are shown in Fig. 13c. Although the application of this thermometer works best for rutiles derived from rocks with rutile–quartz–zircon assemblages, it has been shown that calculations of rutiles from mafic rocks can provide complementary temperature information (Zack and Luvizotto, 2006; Triebold et al., 2007). Calculated formation temperatures for rutiles of the Karaburun samples range from 500 to 950 °C. The major population in all samples, except KAR7, occurs in the range from 600 to 700 °C (42–

61%). High-temperature rutiles (>700 °C) are of minor importance in samples KAR20A (Güvercinlik Formartion), KAR4 (İdecik unit) and the Küçükbahçe Formation but dominate in sample KAR7 (Dikendağı Formation) and are present in great numbers in KAR3 (İdecik unit) and KAR22 (Alandere Formation).

4.4.3. Chrome spinel

Compositional data of detrital chrome spinel were obtained from 122 single grains of the Upper Palaeozoic Küçükbahçe and Alandere formations and the Lower Triassic Gerence Formation. Analysed grains have TiO_2 concentrations <0.8 wt.% with variable Al_2O_3 contents of 2–37 wt.% (Fig. 14a). Cr-spinel from the Upper Palaeozoic formations mostly scatter in the lower area of the diagram (<0.1 wt.% TiO_2). Many grains from the Alandere Formation reveal MORB peridotite affinity and preferably more chrome spinels of the Küçükbahçe Formation plot in the field of supra-subduction zone (SSZ) peridotites. Grains from the Lower Triassic Gerence Formation form a distinct group, characterised by generally higher TiO_2 and lower Al_2O_3 concentrations. This signature is preferably indicative of island-arc basalts but also mid-ocean ridge basalts to a lesser extent. Calculated Cr# and Mg# values vary between 0.33–0.83 (with one very Cr-rich spinel at 0.94) and 0.25–0.75, respectively (Fig. 14b). Chrome spinel grains from the Upper Palaeozoic samples of the Karaburun Peninsula overlap with reference data of chrome spinels from Upper Palaeozoic and Lower Mesozoic siliciclastic sediments of Chios Island and suggest a mixed (ultra)mafic source of dominant harzburgite and minor lherzolite composition. The chrome spinel composition in the Gerence Formation is more variable in Mg# and a proportion of grains has considerably high Cr# and Mg#, and for the most part they overlap with the field of podiform chromitites. At this point it should be mentioned that chrome spinel grains of this Lower Triassic sample (KAR1) are often euhedral (Fig. 10f), which was not observed in any other population.

5. Discussion

5.1. Tectonic setting

The new dataset from the Karaburun Peninsula provides some important parameters that allow a refined interpretation of the tectonic settings of these sediments. Besides the petrographic and chemical composition of sediments also the zircon population and corresponding age spectra help deciphering the tectonic setting of a basin. Depending on the nature of a sedimentary basin, the magmatic and tectonic activity and the extent of erosion are of variable intensity. These processes are the main factors controlling the supply and preservation potential of zircon in sedimentary rocks. Cawood et al. (2012) used the difference between crystallisation ages of detrital zircon and depositional age of sediments to infer information on the tectonic setting of a basin. Following their approach, it allows to discriminate three settings: i) Convergent settings, including basins within supra-subduction zone (SSZ) settings, extending from trench to back-arc that exhibit high quantities of zircons with ages close to the depositional age. ii) In contrast, zircon age spectra with large differences between crystallisation and depositional age and negligible amount of grains with ages close to the depositional age (<150 Ma) are indicative of extensional settings. iii) Basins resulting from continental collision are identified by intermediate zircon spectra with low proportion of grains with ages approximating the depositional age, but moderate amount of zircons having ages within 150 Ma of the sedimentation age. Zircon data of sedimentary rocks from the Karaburun Peninsula and the islands of Inousses and Chios are shown in Fig. 15, following the approach of Cawood et al. (2012). Samples from the Güvercinlik Formation have a high amount of zircon (48%) with ages within 150 Ma of the host sediment, suggesting deposition in convergent or more probably a collisional setting. A similar pattern is revealed by sediments of the Gerence Formation with a very high proportion of grains (>90%) with ages within 200 Ma of the age of the sediment, indicative of collisional or convergent settings. It should be mentioned that the number of detrital zircons is comparatively low (n = 51) – a higher number of zircons would potentially yield a clearer result. In contrast, the Ladinian–Carnian İdecik unit shows highest deviation of the youngest zircon population and depositional age – only 7% of all grains are within a 150 Ma difference – and (almost) match the criteria for extensional settings. Samples from the Küçükbahçe,

Dikendağı and Alandere formations have variable amounts of zircons with ages within 150 Ma of the depositional age (24%, 12% and 28%, respectively) and plot in the field of collisional settings. Sample KAR7 from the Dikendağı Formation is illustrated in a separate graph because its petrographic and geochemical features, and unimodal detrital zircon spectrum (400–450 Ma) are of special character. A similar unimodal spectrum (350–400 Ma) is revealed by zircons of the Gerence Formation, suggesting a collisional or convergent setting. Data from sedimentary rocks of Chios are plotted for comparison, but they are of limited validity due to the very low number of data points (n = 27 and n = 23). However, their patterns suggest deposition in a collisional setting. The zircon population of Inousses is comparable to the Küçükbahçe and Alandere formations of Karaburun, thus suggesting a collisional setting. One should keep in mind that this approach can be very sensitive to the accuracy to which the depositional ages are known. This is of special importance for the interpretation of basins with extensive syndepositional magmatic activity (Cawood et al., 2012).

Deciphering the tectonic settings of depositional basins has proven to be a challenging task, and the use of complementary techniques (e.g., petrography, geochemistry, geochronology) is essential for well-founded interpretations. For instance, Armstrong-Altrin and Verma (2005) highlighted significant problems with conventional well-established tectonic discrimination diagrams. Proposed plots of Bhatia (1983) were evaluated using Miocene to Recent sandstones from known tectonic settings and turned out to yield unsatisfactory results with low rates of success, varying from 0 to 62%. A more recent study by Verma and Armstrong-Altrin (2016) tested the performance of the Roser and Korsch (1986) diagram with respect to grain-size dependency. For fine-grained samples from active margins a success rate of nearly 72% was yielded whereas only 14% of coarse-grained sandstones were successfully classified. Performance of the diagram was even worse for passive margin environments with rates of success between 17% and 39%, respectively. The authors suggest the chosen database for establishment of the diagram was not representative of a worldwide average and might be a major source of error. New discrimination function-based diagrams proposed

by Verma and Armstrong-Altrin (2013, 2016) (Fig. 10b–d) were tested on a large number of Neogene and Quaternary siliciclastic sediments from known tectonic settings and yielded very high success rates of 85 to 94% and 87 to 97%, respectively. A compilation of discrimination diagrams used for the present study is given in Fig. 16 and points out remarkably different results. In spite of the great performance of the Verma and Armstrong-Altrin's plots, discrimination of samples from Karaburun Peninsula and Chios Island, especially the Upper Palaeozoic sandstones of the Küçükbahçe and Dikendağı formations is problematic and to some extent contradictory. Verma and Armstrong-Altrin (2013, 2016) state that their approach has shown to be robust against weathering and diagenetic processes but potential uncertainty might arise from other factors. For instance, the diagram published in 2013 (Fig. 16c) was successfully tested on old, Precambrian rocks, but the effect of grain size is not discussed. In contrast, the database for plots published in 2016 (Fig. 16d–e) includes a wide range of mud-, clay-, silt- and sandstones, thus considering grain size but performance was not yet tested on pre-Quaternary rocks.

Within the framework of previous studies on the Karaburun Peninsula the sedimentary units have been interpreted in different ways and the formation and tectonic setting of the mélange unit has been discussed controversially. Kozur (1995, 1998) favour a sedimentary olistostromal origin of the mélange as an accretionary complex with periodic emplacement of olistoliths. Robertson and Pickett (2000) agree with this model but suggest a tectonic rather than a sedimentary formation process. In this model, mélange blocks were produced by shearing of limestones, cherts and a siliciclastic matrix during collisional processes. In another scenario the Palaeozoic successions are interpreted as remnants of an accretionary complex that was exhumed and reworked as olistostromes into a fore-arc basin during Late Carboniferous time (Stampfli et al., 2003). According to Erdoğan et al. (1990, 2000), the Palaeozoic and Triassic successions including Upper Palaeozoic blocks of limestone and chert were related to Triassic rifting and continuous synsedimentary tectonic activities.

Most of the discussed models consider the Palaeozoic silciclastic rocks of the Karaburun and Chios mélange as remnants of an accretionary complex that represents the (first) passive,

then active margin of the Palaeotethyan Ocean. Incipient subduction beneath the either Gondwana or Eurasian margin in Carboniferous times led to the formation of a magmatic-arc and development of a fore-arc basin (Moix et al., 2013). Also the polarity of subduction and palaeoposition of the Chios–Karaburun units during this time period is still a matter of discussion. Some workers favour a position along the northern margin of Gondwana in combination with southward subduction (e.g., Robertson and Pickett, 2000; Robertson and Ustaömer, 2009a; Akal et al., 2011). Comparable units have also been described from the Konya area (south central Turkey) and are interpreted to have been deposited either along the northern margin of Palaeotethys, i.e. southern margin of Eurasia (Eren et al., 2004), or along the southern margin of Palaeotethys, i.e. northern margin of Gondwana (Göncüoğlu et al., 2007; Robertson and Ustaömer, 2009b). Carboniferous arc-type magmatic rocks have been reported from the Simav area (NW Afyon Zone) and were interpreted as evidence for short-lived southward subduction of Palaeotethys beneath the northern Gondwana margin (Candan et al., 2016). In contrast, models proposing a position along the southern Eurasian margin are discussed as well (e.g., Stampfli, 2000; Stampfli et al., 2003; Zanchi et al., 2003; Moix et al., 2008) (Fig. 17) and are supported by this study based on the sedimentary provenance data from Chios Island and the Karaburun Peninsula. Detrital zircons from the Chios–Karaburun units and Inousses island have shown that they share similar provenance and were sourced from basement units located at the southern Eurasian margin during Late Palaeozoic time (Meinhold and Frei, 2008; Meinhold et al., 2008b; Löwen et al., 2017), the exception being two samples from the heterogeneous Dikendağı Formation (see Löwen et al., 2017). Carboniferous foraminiferal fauna with distinct biogeographical affinities to the southern Laurasian shelf support this interpretation (Kalvoda, 2003).

As discussed above, information on the nature of this margin inferred from geochemical data of the Upper Carboniferous–Lower Permian sediments from Karaburun (i.e., Dikendağı and Küçükbahçe formations) is ambiguous. Some of these samples, in particular KAR7 of the Dikendağı Formation, indicate deposition in close proximity to a magmatic-arc source. This is further supported by its petrographic composition (i.e., high amount of lithic volcanic

fragments and large, sub-/euhedral plagioclase crystals) as well as the observed detrital zircon spectra (Fig. 15). Deposition close to a magmatic-arc is also indicated by petrographic analysis of sample KAR27 that has been tentatively assigned to the Küçükbahçe Formation and exhibits high amounts of mafic volcanic fragments. The presence of such fragments is not common and has not been observed in other parts of this formation. This observation in combination with its sample location close to the boundary of the Dikendağı Formation (Fig. 1b), and slightly different zircon spectra (Löwen et al., 2017) make a correct stratigraphic assignment difficult. Geochemical signatures of some Upper Palaeozoic samples are indicative of a passive margin setting (Fig. 16). However, deposition most likely took place spatially separated from each other at an active margin, probably in a continental island-arc environment related to subduction of the Palaeotethys. These successions, forming the present-day stack of units have been tectonically juxtaposed by supposed post-Cretaceous thrusting. Fossil-rich limestones in the upper part of the Alandere Formation mark a shallowing upward trend to reefal conditions in Late Mississippian time. This is in accordance with the supposed evolution of the neighbouring islands of Chios and Inousses (Meinhold et al., 2007).

Transgressive conglomerates at the basal part of the Gerence Formation that is interpreted as synrift sequence (Robertson and Pickett, 2000) unconformably overlie the Palaeozoic successions and mark the end of a period of intensified erosion. Geochemical data of siliciclastic sediments and their petrographic composition with highly abundant fragments of felsic volcanic rocks (Fig. 4) support this interpretation. Shallow water conditions, indicated by shallow macrofauna in Triassic limestones were followed by rapid tectonic subsidence and accompanied volcanic activity (Stampfli et al., 2003). This is documented by Early Triassic I-type granitoid bodies within the Dikendağı Formation that intruded in a subduction influenced setting related to a continental-arc environment (Erkül et al., 2008; Akal et al., 2011). Indication for enhanced volcanic activity during that period can be found elsewhere in the larger study area, e.g., the Serbo-Macedonian Massif, the Pelagonian Zone, the External Hellenides, the Attic-Cycladic zone and the Menderes Massif (e.g., Tomaschek et al., 2001;

Koralay et al., 2001; Bröcker and Pidgeon; Anders et al., 2007; Himmerkus et al., 2009; Zulauf et al., 2015). The presence of a Ladinian–Carnian carbonate platform (i.e., Camiboğazı Formation) documents a return to shallow water conditions that evolved into a siliciclastic dominated system in Late Triassic time. Lithological features of sediments from the Late Triassic Güvercinlik Formation indicate a tidal flat and reefal environment accompanied by sporadic occurrence of evaporitic deposits (Erdoğan et al., 1990). High geochemical and compositional maturity and inferred information from tectonic discrimination diagrams suggest deposition in a passive margin setting.

5.2. Provenance

Unraveling the provenance of Palaeozoic to Early Mesozoic Palaeotethys-related sedimentary rocks of the Karaburun Peninsula is essential for a better understanding of the geodynamic evolution during that period. The analyses of petrographic and bulk-rock chemical compositions and complementary single-grain analyses provide valuable information in this regard. A short summary of the main observations is given in Table 3.

Detrital chrome spinel of sandstones from the Alandere, Küçükbahçe and Gerence formations is attributed to the (former) presence of (ultra)mafic rocks in the surrounding area. At the present time, outcrops of Palaeotethyan ophiolites are rare in the Eastern Mediterranean as they are either not preserved or not exposed, and chemical data from associated chrome spinel are only available from a few occurrences. These include the Elekdağ ophiolite of the Central Pontides in northern Turkey and the Dobromirtsi Ultramafic Massif in south-eastern Bulgaria (Fig. 1a). The compositions of analysed chrome spinel from the Alandere and Küçükbahçe formations are similar to those reported from Upper Palaeozoic and Lower Mesozoic sediments of Chios and do not overlap with chrome spinel derived from the above-mentioned ophiolites (Fig. 14). It is rather likely that these grains were either recycled from older sediments or derived from Late Neoproterozoic ophiolitic bodies of NW Turkey and/or the Balkans as suggested by Meinhold et al. (2007) for detrital chrome spinels from Chios. In contrast, compositional data of chrome spinel from the Lower

Triassic Gerence Formation pinpoint a remarkably different source. Additionally, the euhedral shape of these grains indicates short sedimentary transport implying a very proximal provenance and also excludes recycling of older sedimentary rocks, i.e., underlying formations. Chrome spinel chemistry shows great overlap with grains from the Dobromirtsi Ultramafic Massif of south-eastern Bulgaria and the Elekdağ ophiolite of northern Turkey, but there is no perfect match for one of them (Fig. 14). The observed signatures on the one hand typify grains derived from boninitic rocks related to fore-arc settings during subduction initiation, which is the favoured interpretation for the Elekdağ ophiolite (Ustaömer and Robertson, 1997, 1999; Dönmez et al., 2014). But then they could also be indicative for chrome spinel derived from podiform chromitites that were formed in an intra-oceanic back-arc setting above a supra-subduction zone – a model suggested for chromitites of the Dobromirtsi Ultramafic Massif (González-Jiménez et al., 2012). The lack of a suitable number of reference data and generally low occurrence of Palaeotethys-related ophiolites complicate the approach to unravel the provenance of detrital chrome spinel in Karaburun sediments. Nevertheless, on the basis of the available information we consider Palaeozoic ophiolites of northern Turkey and south-eastern Bulgaria or equivalent occurrences in the SE Europe that are not exposed or not preserved as most likely sources for chrome spinel in the Gerence Formation. This assumption is consistent with a unimodal age spectra of analysed detrital zircons (~80% of all zircons have ages between 350 and 450 Ma) indicating sediment supply from a localised source of mainly Silurian and Devonian age (Löwen et al., 2017). These findings document the existence of an (intra-oceanic) SSZ setting within the Palaeotethys. Ophiolite obduction must have occurred before deposition of the Gerence Formation, and due to the euhedral shaped chrome spinels the ophiolite was likely in very close distance to the depositional site of the Gerence Formation in Early Triassic time. Zr-in-rutile thermometry has shown that a majority of rutile grains were derived from amphibolite- to eclogite-facies rocks and input from granulite-facies lithologies is only documented in a few samples (KAR3, KAR7, KAR22). Additionally, the Cr–Nb composition generally indicates prominent input from felsic lithologies to the siliciclastic rocks of the study area, the exception being analysed

sediments of the Küçükbahçe Formation and one sample (KAR4) of the İdecik unit that exhibit a higher proportion of rutiles from mafic source rocks. This is consistent with the similar detrital zircon spectra of these sediments, further suggesting recycling of Palaeozoic rocks into the İdecik unit or sediment supply by the same source (Löwen et al., 2017). Nonetheless, one should keep in mind the doubtful assignment of sample KAR27. By comparison, observed formation temperatures of detrital rutile from Chios are similar, but grains of the Carboniferous succession were mainly derived from mafic rocks whereas Permian–Carboniferous and Permian–Triassic units record major input from felsic lithologies (Meinhold et al., 2008a). Possible sources of amphibolite- to eclogite-facies rocks were located in the metamorphic basement of the Balkan region including the Sredna Gora Zone and Strandja, Rhodope and Serbo-Macedonian massifs (e.g., Okay et al., 2001; Carrigan et al., 2006). Furthermore, high-grade, granulite-facies metamorphic rocks are documented in the Pelagonian Zone, the Variscan basement of the Sakarya Zone and the eclogite-facies basement of the Menderes Massif (e.g., Candan et al., 2001; Mposkos et al., 2001).

Analyses of garnet from the Alandere Formation has shown that most grains exhibit an intermediate to felsic volcanic provenance and were not supplied by the same source with chrome spinel. Geochemical signatures and abundant mafic volcanic fragments document the importance of (ultra)mafic lithologies in the source area. Garnets of the Triassic formations were predominantly derived from felsic igneous rocks and amphibolite-facies metasediments. The classification scheme does not provide any indication for an ultramafic provenance, implying that garnet and chrome spinel of the Gerence Formation were likely not supplied by a common source. In case of high mature sandstones from the Güvercinlik Formation, material was probably supplied by mainly quartzose, amphibolite-facies metasediments and volcanic rocks of a more distal region.

6. Conclusions

The petrographic and geochemical data presented in our study provide new constraints on the provenance and depositional tectonic setting of sediments from the Karaburun Peninsula that can be summarised as followed:

- Provenance sensitive elements (Cr, Ni, Th, Sc, V) document a predominant felsic character of source lithologies but also indicate considerable amount of mafic components in selected samples.
- Tectonic discrimination diagrams utilizing bulk-rock geochemical data can provide good indication on the tectonic setting of depositional basins, but should be treated with caution. The choice of a representative and extensive database is a key prerequisite for testing these diagrams as their performance can be hampered by insufficient review of age and grain-size effects of analysed samples. Additionally, complementary techniques and the regional geological context should not be disregarded for conclusive interpretation of these results.
- Mineral chemical analysis of rutile and abundant sedimentary lithic fragments revealed the major importance of amphibolte- to eclogite-facies sources for sediments throughout the whole stratigraphic sequence of the Karaburun Peninsula. Material was predominantly derived from felsic lithologies, but detritus of mafic provenance was supplied to some extent.
- Euhedral chrome spinels from the Lower Triassic Gerence Formation document the existence of an (intra-oceanic) SSZ setting within the Palaeotethys. Related ophiolites were present in proximity to the depositional site of the Gerence Formation and supplied detritus. We assume that these Palaeozoic ophiolites were probably located in northern Turkey or the Balkans but are not exposed or preserved anymore. Deciphering a more accurate provenance of this material is hindered by the lack of reference data (i.e., mineral chemical data of chrome spinel) from other Palaeozoic (ultra)mafic bodies.

- We assume that most of the Upper Palaeozoic successions of the Karaburun Peninsula were (contemporaneously) deposited along the southern active Eurasian margin. Low textural and compositional maturity indicate relatively proximal provenance and the presence of a nearby volcanic-arc, probably related to northward subduction of Palaeotethys.

Acknowledgements

We gratefully acknowledge financial support by the German Research Foundation (DFG grant ME 3882/3-1) and the Göttingen University start-up funding for young academics (grant to GM). We thank Gerald Hartmann for XRF analysis, Klaus Simon for ICP-MS analysis, and Andreas Kronz for providing access to the EMPA. Günay Kurtuluş kindly provided chrome spinel reference data of the Elekdağ ophiolite. Constructive reviews were provided by Shane Tyrrell and Mehmet Cemal Göncüoğlu and are greatly appreciated.

Appendix A. Supplementary data

Supplementary data associated with this article can be found in the online version at http://xxxxx

- Table S1: Main and trace element data from XRF and ICP-MS analyses
- Table S2: Operating conditions of the electron microprobe analyzer (EPMA)
- Table S3: Mineral chemical data from EMPA

References

Akal, C., Koralay, O., Candan, O., Oberhänsli, R., Chen, F., 2011. Geodynamic significance of the Early Triassic Karaburun granitoid (Western Turkey) for the opening history of Neo-Tethys. Turkish Journal of Earth Sciences 20, 255–271.

Anders, B., Reischmann, T., Kostopoulos, D., 2007. Zircon geochronology of basement rocks from the Pelagonian Zone, Greece: constraints on the pre-Alpine evolution of the westernmost Internal Hellenides. International Journal of Earth Sciences 96, 639–661.

Bauluz, B., Mayayo, M.J., Fernandez-Nieto, C., Lopez, J.M.G., 2000. Geochemistry of Precambrian and Paleozoic siliciclastic rocks from the Iberian Range (NE Spain): implications for source-area weathering, sorting, provenance, and tectonic setting. Chemical Geology 168, 135–150.

Besenecker, H., Dürr, S., Herget, G., Jacobshagen, V., Kauffmann, G.L., Lüdtke, G., Roth, W., Tietze, K.W., 1968. Geologie von Chios (Ägäis). Geologica et Palaeontologica 2, 121–150.

Bhatia, M.R., 1983. Plate tectonics and geochemical composition of sandstones. Journal of Geology 91, 611–627.

Bhatia, M.R., Crook, A.W., 1986. Trace element characteristics of graywackes and tectonic setting discrimination of sedimentary basins. Contributions to Mineralogy and Petrology 92, 181–193.

Boynton, W.V., 1984. Geochemistry of the rare earth elements: Meteorite studies. In: Henderson, P. (Eds.), Geochemistry of the Rare Earth Elements. Elsevier, pp. 63–114.

Bracciali, L., Marroni, M., Pandolfi, L., Rocchi, S., 2007. Geochemistry and petrography of Western Tethys Cretaceous sedimentary covers (Corsica and Northern Apennines): From source areas to configuration of margins. In: Arribas, J., Critelli, S., Johnsson, M.J. (Eds.), Sedimentary Provenance and Petrogenesis: Perspectives from Petrography and Geochemistry. Geological Society of American, Special Paper 420, pp. 73–93.

Brinkmann, R., Flügel, E., Jacobshagen, V., Lechner, H., Rendel, B., Trick, P., 1972. Trias, Jura und Unterkreide der Halbinsel Karaburun (West Anatolien). Geologica Palaeontologica 6, 139–150.

Bröcker, M., Pidgeon, R.T., 2007. Protolith ages of meta-igneous and metatuffaceous rocks from the Cycladic Blueschist unit, Greece: results of a reconnaissance U–Pb zircon study. Journal of Geology 115, 83–98.

Çakmakoğlu, A., Bilgin, Z., 2006. Pre-Neogene stratigraphy of the Karaburun Peninsula (W

of İzmir Turkey). Bulletin of the Mineral Research and Exploration Institute of Turkey 132, 33–61.

Candan, O., Dora, O., Oberhänsli, R., Çetinkaplan, M., Partzsch, J., Warkus, F., Dürr, S., 2001. Pan-African high-pressure metamorphism in the Precambrian basement of the Menderes Massif, western Anatolia, Turkey. International Journal of Earth Sciences 89, 793–811.

Candan, O., Akal, C., Koralay, O.E., Okay, A.I., Oberhänsli, R., Prelević, D., Mertz-Kraus, R., 2016. Carboniferous granites on the northern margin of Gondwana, Anatolide-Tauride Block, Turkey – Evidence for southward subduction of Paleotethys. Tectonophysics 683, 349–366.

Caracciolo, L., Critelli, S., Cavazza, W., Meinhold, G., von Eynatten, H., Manetti, P., 2015. The Rhodope Zone as a primary sediment source of the southern Thrace basin (NE Greece and NW Turkey): evidence from detrital heavy minerals and implications for central-eastern Mediterranean palaeogeography. International Journal of Earth Sciences 104, 815–832.

Cawood, P.A., Hawkesworth, C.J., Dhuime, B., 2012. Detrital zircon record and tectonic setting. Geology 40, 875–878.

Cookenboo, H.O., Bustin, R.M., Wilks, K.R., 1997. Detrital chromian spinel compositions used to reconstruct the tectonic setting of provenance: implications for orogeny in the Canadian Cordillera. Journal of Sedimentary Research 67, 116–123.

Cullers, R.L., 1994. The controls on the major and trace element variation of shales, siltstones, and sandstones of Pennsylvanian-Permian age from uplifted continental blocks in Colorado to platform sediment in Kansas, USA. Geochimica et Cosmochimica Acta 58, 4955–4972.

Cullers, R.L., Graf, J.L., 1984. Rare earth elements in igneous rocks of the continental crust: intermediate and silicic rocks, ore petrogenesis. In: Henderson, P. (Ed.), Rare earth

element geochemistry. Elsevier, Amsterdam, pp. 275–312.

Deer, W.A., Howie, R.A., Zussman, J., 1992. An Introduction to the Rock-Forming Minerals. Longman Group Ltd., Harlow, UK (712 pp.).

Dickinson, W.R., Beard, L.S., Brakenridge, G.R., Erjavec, J.L., Ferguson, R.C., Inman, K.F., Knepp, R.A., Lindberg, F.A., Ryberg, P.T., 1983. Provenance of North American Phanerozoic sandstones in relation to tectonic setting. Geological Society of America Bulletin 94, 222–235.

Dönmez, C., Keskin, S., Günay, K., Çolakoğlu, A.O., Çiftçi, Y., Uysal, I., Türkel, A., Yıldırım, N., 2014. Chromite and PGE geochemistry of the Elekdağ Ophiolite (Kastamonu, Northern Turkey): Implications for deep magmatic processes in a supra-subduction zone setting. Ore Geology Reviews 57, 216–228.

Engel, M., Reischmann, T., 1998. Single zircon geochronology of orthogneisses from Paros, Greece. Bulletin of the Geological Society of Greece 32, 91–99.

Ercan, T., Türkecan, A., Satır, M., 2000. Karaburun Yaramadasının Neojen volkanizması [Neogene volcanism of Karaburun Peninsula]. Proceedings, Cumhuriyetin 75. Yıldönümü Yerbilimleri ve Madencilik Kongresi Bildiriler Kitabı. Mineral Research Exploration Institute of Turkey, Ankara, pp. 1–18.

Erdoğan, B., Altıner, D., Güngör, T., Özer, S., 1990. Stratigraphy of Karaburun peninsula. Bulletin of the Mineral Research and Exploration Institute of Turkey 111, 1–23.

Erdoğan, B., Güngör, T., Özer, S., 2000. Stratigraphy of Karaburun Peninsula Excursion Guide. International Earth Science Colloquium on the Aegean Region (IESCA) 2000, İzmir, pp. 1–32.

Eren ,Y., Kurt, H., Rosselet, F., Stampfli, G.M., 2004. Palaeozoic deformation and magmatism in the northern area of the Anatolide block (Konya), witness of the Palaeotethys active margin. Eclogae Geologicae Helvetiae 97, 293–306.

Garver, J.I., Royce, P.R., Smick, T.A., 1996. Chromium and nickel in shale of the Taconic

foreland: a case study for the provenance of fine-grained sediments with an ultramafic source. Journal of Sedimentary Research 66, 100–106.

Göncüoğlu, M.C., Çapkınoğlu, Ş., Gürsu, S., Noble, P., Turhan, N., Tekin, U.K., Okuyucu, C., Göncüoğlu, Y., 2007. The Mississippian in the Central and Eastern Taurides (Turkey): constraints on the tectonic setting of the Tauride–Anatolide Platform. Geologica Carpathica 58, 427–442.

González-Jiménez, J.M., Colás, V., Sergeeva, I., Griffin, W.L., O'Reilly, S.Y., Gervilla, F., Kerestedjian, T., Fanlo, I., Locmelis, M., Peasron, N., Belousova, E., 2012. Back-Arc Origin for Chromitites of the Dobromirtsi Ultramafic Massif. Revista de la Sociedad Española de Mineralogía 16, 240–241.

González-Jiménez, J.M., Locmelis, M., Belousova, E., Griffin, W.L., Gervilla, F., Kerestedjian, T., O'Reilly, S.Y., Pearson, N.J., Sergeeva, I., 2015. Genesis and tectonic implications of podiform chromitites in the metamorphosed ultramafic massif of Dobromirtsi (Bulgaria). Gondwana Research 27, 555–574.

Gromet, L.P., Dymek, R.F., Haskin, L.A., Korotev, R.L., 1984. The ''North American Shale Composite": its composition, major and trace element characteristics. Geochimica et Cosmochimica Acta 48, 2469–2482.

Herron, M.M., 1988. Geochemical classification of terrigenous sands and shales from core or log data. Journal of Sedimentary Petrology 58, 820–829.

Himmerkus, F., Reischmann, T., Kostopoulos, D., 2009. Triassic rift-related meta-granites in the internal Hellenides, Greece. Geological Magazine 146, 252–265.

Hofmann, A., Bolhar, R., Dirks, P., Jelsma, H., 2003. The geochemistry of Archean shales derived from a Mafic volcanic sequence, Belingwe greenstone belt, Zimbabwe: provenance, source area unroofing and submarine versus subaerial weathering. Geochimica et Cosmochimica Acta 67, 421–440.

Ingersoll, R.V., Bullard, T.F., Ford, R.L., Grimm, J.P., Pickle, J.D., Sares, S.W., 1984. The

effect of grain size on detrital modes: a test of the Gazzi-Dickinson point-counting method. Journal of Sedimentary Petrology 54, 103–116.

Jacobshagen, V., 1986. Geologie von Griechenland. Gebrüder Borntraeger, Berlin (363 pp.).

Kalafatçıoğlu, A., 1961. A geological study in the Karaburun Peninsula. Bulletin of the Mineral Research and Exploration Institute of Turkey 56, 40–49.

Kalvoda, J., 2003. Carboniferous foraminiferal paleobiogeography in Turkey and its implications for plate tectonic reconstructions. Rivista Italiana di Paleontologia e Stratigrafia 109, 255–266.

Kamenetsky, V.S., Crawford, A.J., Meffre, S., 2001. Factors controlling chemistry of magmatic spinel: an empirical study of associated olivine, Cr-spinel and melt inclusions from primitive rocks. Journal of Petrology 42, 655–671.

Koralay, O.E., Satir, M., Dora, O.Ö., 2001. Geochemical and geochronological evidence for Early Triassic calc-alkaline magmatism in the Menderes Massif, western Turkey. International Journal of Earth Sciences 89, 822–835.

Kozur, H., 1995. New stratigraphic results on the Palaeozoic of the Western parts of the Karaburun Peninsula, Western Turkey. In: Pişkin, O., Ergün, M., Savaşçin, M.Y., Tarcan, G., (Eds.), Proceedings of International Earth Sciences Colloquium on the Aegean Region, İzmir, pp. 289–308.

Kozur, H., 1997. First discovery of Muellerisphaerida (inc. sedis) and *Eoalbaillella* (Radiolaria) in Turkey and the age of the siliciclastic sequence (clastic series) in Karaburun peninsula. Freiberger Forschungshefte-Reihe C, Geowissenschaften 466, 33–59.

Kozur, H., 1998. The age of the siliciclastic series (“Karareis Formation”) of the western Karaburun peninsula, western Turkey. In: Szaniawski, H. (Eds.), Proceedings of the Sixth European Conodont Symposium (ECOS VI), Palaeontologia Polonica 58, pp. 171–189.

Krippner, A., Meinhold, G., Morton, A.C., von Eynatten, H., 2014. Evaluation of garnet discrimination diagrams using geochemical data of garnets derived from various host rocks. Sedimentary Geology 306, 36–52.

Krippner, A., Meinhold, G., Morton, A.C., Russell, E., von Eynatten, H., 2015. Grain-size dependence of garnet composition revealed by provenance signatures of modern stream sediments from the western Hohe Tauern (Austria). Sedimentary Geology 321, 25–38.

Krippner, A., Meinhold, G., Morton, A.C., Schönig, J., von Eynatten, H., 2016. Heavy minerals and garnet geochemistry of stream sediments and bedrocks from the Almklovdalen area, Western Gneiss Region, SW Norway: implications for provenance analysis. Sedimentary Geology 336, 96–105.

Löwen, K., Meinhold, G., Güngör, T., Berndt, J., 2017. Palaeotethys-related sediments of the Karaburun Peninsula, western Turkey: Constraints on provenance and stratigraphy from detrital zircon geochronology. International Journal of Earth Sciences 106, 2771–2796.

Lužar-Oberiter, B., Mikes, T., von Eynatten, H., Babić, L., 2009. Ophiolitic detritus in Cretaceous clastic formations of the Dinarides (NW Croatia): evidence from Cr-spinel chemistry. International Journal of Earth Sciences 98, 1097–1108.

Mange, M.A., Morton, A.C., 2007. Geochemistry of heavy minerals. In: Mange, M.A., Wright, D.T. (Eds.), Heavy Minerals in Use. Developments in Sedimentology 58. Elsevier, Amsterdam, pp. 345–391.

McBride, E.F., 1963. A classification of common sandstones. Journal of Sedimentary Research 33, 664–669.

McLennan, S.M., 1989. Rare earth elements in sedimentary rocks: influence of provenance and sedimentary processes. In: Lipin, B.R., McKay, G.A. (Eds.), Geochemistry and Mineralogy of Rare Earth Elements. Reviews in Mineralogy 21, pp. 169–200.

McLennan, S.M., Hemming, S., McDaniel, D.K., Hanson, G.N., 1993. Geochemical approaches to sedimentation, provenance, and tectonics. In: Johnsson, M.J., Basu, A. (Eds.), Processes Controlling the Composition of Clastic Sediments. Geological Society of America, Special Papers 284, pp. 21–40.

Meinhold, G., 2010. Rutile and its applications in earth sciences. Earth-Science Reviews 102, 1–28.

Meinhold, G., Frei, D., 2008. Detrital zircon ages from the islands of Inousses and Psara, Aegean Sea, Greece: constraints on depositional age and provenance. Geological Magazine 145, 886–891.

Meinhold, G., Kostopoulos, D., Reischmann, T., 2007. Geochemical constraints on the provenance and depositional setting of sedimentary rocks from the islands of Chios, Inousses and Psara, Aegean Sea, Greece: implications for the evolution of Palaeotethys. Journal of the Geological Society 164, 1145–1163.

Meinhold, G., Anders, B., Kostopoulos, D., Reischmann, T., 2008a. Rutile chemistry and thermometry as provenance indicator: an example from Chios Island, Greece. Sedimentary Geology 203, 98–111.

Meinhold, G., Reischmann, T., Kostopoulos, D., Lehnert, O., Matukov, D., Sergeev, S., 2008b. Provenance of sediments during subduction of Palaeotethys: Detrital zircon ages and olistolith analysis in Palaeozoic sediments from Chios Island, Greece. Palaeogeography, Palaeoclimatology, Palaeoecology 263, 71–91.

Moix, P., Beccaletto, L., Kozur, H.W., Hochard, C., Rosselet, F., Stampfli, G.M., 2008. A new classification of the Turkish terranes and sutures and its implication for the paleotectonic history of the region. Tectonophysics 451, 7–39.

Moix, P., Vachard, D., Allibon, J., Martini, R., Wernli, R., Kozur, H.W., Stampfli, G.M., 2013. Palaeotethyan, Neotethyan and Huglu-Pindos series in the Lycian Nappes (SW Turkey): geodynamical implications. In: Tanner, L.H., Spielmann, J.A., Lucas, S.G. (Eds.), The Triassic System. New Mexico Museum of Natural History and Science, New Mexico, pp.

401–444.

Morton, A.C., 1985. A new approach to provenance studies: electron microprobe analysis of detrital garnets from Middle Jurassic sandstones of the northern North Sea. Sedimentology 32, 553–566.

Mposkos, E., Kostopoulos, D.K., Krohe, A., 2001. Low-P/high-T pre-Alpine metamorphism and medium-P Alpine overprint of the Pelagonian Zone documented in high-alumina metapelites from the Vernon Massif, western Macedonia, northern Greece. Bulletin of the Geological Society of Greece 34, 949–958.

Okay, A.I., Tüysüz, O., 1999. Tethyan sutures of northern Turkey. In: Durand, B., Jolivet, L., Horivath, F., Séranne, M. (Eds.), The Mediterranean Basin: Tertiary extension within the Alpine Orogen. Geological Society of London, Special Publications 156, pp. 475–515.

Okay, A.I., Satır, M., Tüysüz, O., Akyüz, S., Chen, F., 2001. The tectonics of the Strandja Massif: late-Variscan and mid-Mesozoic deformation and metamorphism in the Northern Aegean. International Journal of Earth Sciences 90, 217–33.

Okay, A.I., Satır, M., Siebel, W., 2006. Pre-Alpide Palaeozoic and Mesozoic orogenic events in the Eastern Mediterranean region. In: Gee, D.G., Stephenson, R.A. (Eds.), European Lithosphere Dynamics. Geological Society of London, Memoirs 32, pp. 389–405.

Özmen, F., Reischmann, T., 1999. The age of the Sakarya continent in W Anatolia: implications for the evolution of the Aegean region. Journal of Conference Abstracts 4, 805.

Pagé, P., Barnes, S.J., 2009. Using trace elements in chromites to constrain the origin of podiform chromitites in the Thetford Mines Ophiolite, Québec, Canada. Economic Geology 104, 997–1018.

Philippson, A., 1911. Reisen und Forschungen im westlichen Kleinasien, 2. Heft: Ionien und das westliche Lydien. Petermanns geographische Mitteilungen, Ergänzungsheft 172, 1–100.

Pober, E., Faupl, P., 1988. The chemistry of detrital chromian spinels and its implications for the geodynamic evolution of the Eastern Alps. Geologische Rundschau 77, 641–670.

Reischmann, T., 1998. Pre-alpine origin of tectonic units from the metamorphic complex of Naxos, Greece, identified by single Pb/Pb dating. Bulletin of the Geological Society of Greece 32, 101–111.

Robertson, A.H.F., Pickett, E.A., 2000. Palaeozoic–Early Tertiary Tethyan Evolution of Mmélanges, Rift and Passive Margin Units in the Karaburun Peninsula (western Turkey) and Chios Island (Greece). In: Bozkurt, E., Winchester, J.A., Piper, J.D.A. (Eds.), Tectonic and magmatism in Turkey and the surrounding area. Geological Society of London, Special Publications 173, pp. 43–82.

Robertson, A.H.F., Ustaömer, T., 2009a. Upper Palaeozoic subduction/accretion processes in the closure of Palaeotethys: Evidence from the Chios Melange (E Greece), the Karaburun Melange (W Turkey) and the Teke Dere Unit (SW Turkey). Sedimentary Geology 220, 29–59.

Robertson, A.H.F., Ustaömer, T., 2009b. Formation of the Late Palaeozoic Konya Complex and comparable units in southern Turkey by subduction–accretion processes: Implications for the tectonic development of Tethys in the Eastern Mediterranean region. Tectonophysics 473, 113–148.

Roser, B.P., Korsch, R.J., 1986. Determination of tectonic setting of sandstone–mudstone suites using SiO_2 content and K_2O/Na_2O ratio. Journal of Geology 94, 635–650.

Rudnick, R.L., Gao, S., 2003. Composition of the continental crust. In: Rudnick, R., Holland, H.D., Turekian, K.K. (Eds.), Treatise on Geochemistry 3, pp. 1–64.

Şengör, A.M.C., Yılmaz, Y., Sungurlu, O., 1984. Tectonics of the Mediterranean Cimmerides: nature and evolution of the western termination of Palaeo-Tethys. In: Dixon, J.E., Robertson, A.H.F., (Eds.), The geological evolution of the eastern Mediterranean. Geological Society of London, Special Publications 17, pp. 77–112.

Stampfli, G.M., 2000. Tethyan oceans. In: Bozkurt, E., Winchester, J.A., Piper, J.D.A. (Eds.), Tectonics and magmatism in Turkey and the surrounding area. Geological Society of London, Special Publications 173, pp. 1–23.

Stampfli, G.M., Borel, G., 2002. A plate tectonic model for the Paleo- zoic and Mesozoic constrained by dynamic plate boundaries and restored synthetic oceanic isochrons. Earth and Planetary Science Letters 196, 17–33.

Stampfli, G.M., Hochard, C. Vérard, C., Wilhem, C., von Raumer, J., 2013. The formation of Pangea. Tectonophysics 593, 1–19.

Stampfli, G.M., Vavassis, I., De Bono, A., Rosselet, F., Matti, B., Bellini, M., 2003. Remnants of the Paleotethys oceanic suture-zone in the western Tethyn area. In: Cassinis, G., (Ed.), Stratigraphic and Structural Evolution on the Late Carboniferous to Triassic Continental and Marine Successions in Tuscany (Italy): Regional Reports and General Correlation. Bolletino della Società Geologica Italiana vol. speciale 2, pp. 1–23.

Taylor, S.R., McLennan, S.M., 1985. The continental crust: its composition and evolution. Blackwell Scientific Publications, Oxford (312 pp.).

Tomaschek, F., Kennedy, A., Keay, S., Ballhaus, C., 2001. Geochronological constraints on Carboniferous and Triassic magmatism in the cyclades: SHRIMP U–Pb ages of zircons from Syros, Greece. Journal of Conference Abstracts 6, 315.

Tomkins, H.S., Powell, R., Ellis, D.J., 2007. The pressure dependence of the zirconium-in-rutile thermometer. Journal of Metamorphic Geology 25, 703–713.

Triebold, S., von Eynatten, H., Luvizotto, G.L., Zack, T., 2007. Deducing source rock lithology from detrital rutile geochemistry: an example from the Erzgebirge, Germany. Chemical Geology 244, 421–436.

Triebold, S., von Eynatten, H., Zack, T., 2012. A recipe for the use of rutile in sedimentary provenance analysis. Sedimentary Geology 282, 268–275.

Turpaud, P., Reischmann, T., 2010. Characterisation of igneous terranes by zircon dating:

implications for UHP occurrences and suture identification in the Central Rhodope, northern Greece. International Journal of Earth Sciences 99, 567–591.

Ustaömer, T., Robertson, A.H.F., 1997. Tectonic-sedimentary evolution of the north Tethyan margin in the Central Pontides of northern Turkey. In: Robinson, A.G., (Ed.), Regional and Petroleum Geology of the Black Sea and Surrounding Region. American Association of Petroleum Geologists Memoirs 68, 255–290.

Ustaömer, T., Robertson, A.H.F., 1999. Geochemical evidence used to test alternative plate tectonic models for pre-Upper Jurassic (Paleo-Tethyan) units in the Central Pontides, N. Turkey. Geological Journal 34, 25–54.

Ustaömer, T., Ustaömer, P.A., Robertson, A.H.F., Gerdes, A., 2016. Implications of U–Pb and Lu–Hf isotopic analysis of detrital zircons for the depositional age, provenance and tectonic setting of the Permian–Triassic Palaeotethyan Karakaya Complex, NW Turkey. International Journal of Earth Sciences 105, 7–38.

Verma, S.P., Armstrong-Altrin, J.S., 2013. New multi-dimensional diagrams for tectonic discrimination of siliciclastic sediments and their application to Precambrian basins. Chemical Geology 355, 117–133.

Verma, S.P., Armstrong-Altrin, J.S., 2016. Geochemical discrimination of siliciclastic sediments from active and passive margin settings. Sedimentary Geology 332, 1–12.

Wright, W.I., 1938. The composition and occurrence of garnets. American Mineralogist 23, 436–449.

Xypolias, P., Dörr, W., Zulauf, G., 2006. Late Carboniferous plutonism within the pre-Alpine basement of the External Hellenides (Kithira, Greece): evidence from U-Pb zircon dating. Journal of the Geological Society, London 163, 539–547.

Zack, T., Luvizotto, G.L., 2006. Application of rutile thermometry to eclogites. Mineralogy and Petrology 88, 69–85.

Zanchi, A., Garzanti, E., Larghi, C., Gaetani, M., 2003. The Variscan orogeny in Chios (Greece): Carboniferous accretion along a Palaeotethyan active margin. Terra Nova 15, 213–223.

Zulauf, G., Dörr, W., Fisher-Spurlock, S.C., Gerdes, A., Chatzaras, V., Xypolias, P., 2015. Closure of the Paleotethys in the external Hellenides: Constraints from U–Pb ages of magmatic and detrital zircons (Crete). Gondwana Research 28, 642–667.

Zulauf, G., Dörr, W., Krahl, J., Lahaye, Y., Chatzaras, V., Xypolias, P., 2016. U–Pb zircon and biostratigraphic data of high-pressure/low-temperature metamorphic rocks of the Talea Ori: tracking the Paleotethys suture in central Crete, Greece. International Journal of Earth Sciences 105, 1901–1922.

Tables

Table 1 GPS coordinates of sample locations and summary of conducted analyses

Table 2 Mineralogical composition and point counting results of sediments from the Karaburun Peninsula

Table 3 Main observations from petrography, geochemistry and composition of heavy minerals

Figure captions

Fig. 1 (a) Simplified tectonic map of the Eastern Mediterranean region (compiled and modified after Jacobshagen, 1986; Okay and Tüysüz, 1999; Okay et al., 2006). The locations of the Dobromirtsi and Elekdağ ophiolite occurrences are after González-Jiménez et al. (2015) and Dönmez et al. (2014), respectively. (b) Simplified geological map of the study area with sample locations. The Karaburun map is modified after Çakmakoğlu and Bilgin (2006) and the

Inousses map is modified after Meinhold et al. (2007).

Fig. 2 Palaeozoic to Jurassic tectono-stratigraphic section of the Karaburun Peninsula (modified after Löwen et al., 2017). For simplification, the ?Late Permian Tekedağı Formation, consisting of bioclastic limestone, dolomitic limestone, partly oolitic/pisolitic, and limestone with sandstone, siltstone, and marl interfingers (Çakmakoğlu and Bilgin 2006), is not shown here. The Tekedağı Formation is only present in a small area to the NW of Gerence Bay. This formation probably correlates with the stratigraphically younger part of the Permian limestones from the allochthonous Upper Unit of Chios Island. Blocks / olistoliths in the Palaeozoic succession have been described by Kozur (1998) and Robertson and Ustaömer (2009a). (For interpretation of the reference to colour in this figure legend, the reader is referred to the web version of this article.)

Fig. 3 (a) QFL diagram for lithological classification (after McBride, 1963). (b) Ternary QFL plot for discrimination of tectonic settings (after Dickinson et al., 1983). (c) Chemical classification scheme for siliciclastic sediments (after Herron, 1988).

Fig. 4 Overview of petrographic analysis of sediments from the Karaburun Peninsula. (a) Percentage of quartz, feldspar and lithic fragments resulting from point couting. (b) Degree of sorting (1 – poorly sorted, 2 – moderately sorted, 3 – well sorted, 4 – very well sorted) and rounding (1 – angular, 2 – subangular, 3 – subrounded, 4 – rounded) were used to estimate maturity. (c) Estimated average grain size.

Fig. 5 Selection of photomicrographs (cross-polarised light) of studied sediments from the Karaburun Peninsula. (a) Polysynthetic twinning in inclusion-rich plagioclase (Küçükbahçe Formation). (b) Perthitic exsolution lamellae of plagioclase (albite) in K-feldspar (Küçükbahçe Formation). (c) Overview

showing the texture of sandstone from the Dikendağı Formation. Main composition is monocrystalline quartz with minor feldspar, mica and calcite. (d) Large, angular plagioclase crystals and lithic fragments in an arkosic sandstone (Dikendağı Formation). (e) Overview photograph of well-rounded and poorly-sorted grains with predominantly quartzitic composition (İdecik unit). (f) Myrmekitic intergrowth of quartz in plagioclase cut by calcite veins (Gerence Formation).

Fig. 6 Compilation of photomicrographs showing the main lithic fragments of studied sediments from the Karaburun Peninsula (cross-polarised light). (a) Mafic volcanic fragment (Lv) with plagioclase laths and needles (Alandere Formation). (b) Lithic volcanic fragment mainly composed of plagioclase (Dikendağı Formation). (c) Coarse-grained, altered fragment derived from a mafic volcanic rock (Dikendağı Formation). (d) Low-grade metasedimentary (mica-schist; Lms) and quartzitic fragments (Ls) (Küçükbahçe Formation). (e) Chert fragment (Lc) (Küçükbahçe Formation) (f) Fine-grained volcanic fragment with plagioclase laths and needles (İdecik unit). (g) Coarse-grained volcanic lithic fragment including plagioclase laths (Gerence Formation). (h) Fragments of mica-schist squeezed in intergranular spaces and chert (Güvercinlik Formation).

Fig. 7 Correlation diagrams of SiO_2, TiO_2, Na_2O, Fe_3O_3t and CaO versus Al_2O_3 and CaO versus LOI.

Fig. 8 Chondrite-normalised REE diagrams for samples from the Karaburun Peninsula and the islands of Chios and Inousses. Grey shaded areas indicate total range of data from the Karaburun Peninsula. Normalising values from Boynton (1984). UCC and PAAS data from Rudnick and Gao (2003) and McLennan (1989), respectively. (For interpretation of the reference to colour in this figure legend, the reader is referred to the web version of this article).

Fig. 9 UCC-normalised multielement diagrams for samples from the Karaburun Peninsula. Grey shaded areas indicate total range of data. Normalising values from Rudnick and Gao (2003).

Fig. 10 Discrimination diagrams for identifying an (ultra)mafic provenance. (a) Cr/V versus Y/Ni diagram after McLennan et al. (1993). (b) Cr versus Ni diagram and (c) Cr/Ni ratios. High concentrations of Cr (>150 ppm) and Ni (>100 ppm) combined with Cr/Ni ratios ranging from 1.3 to 1.5 are indicative of an ultramafic provenance; Cr/Ni ratios of 2 and greater typify an input of mafic volcanic rocks (Garver et al., 1996). Abbreviations: *sp* = presence of Cr-spinel, observed in thin section and/or heavy mineral concentrate; P–T = Permian–Triassic; C–P = Carboniferous–Permian; UP = Upper Palaeozoic. (d) Ternary Ni–V–Th×10 diagram for source rock discrimination after Bracciali et al. (2007). Grey shaded areas represent source rock endmembers. (e) Th/Sc versus Cr/Th diagram. Felsic sources tend towards enrichement of incompatible elements (Th) and mafic rocks have higher concentrations of compatible elements (Cr, Sc). (f) Photomicrographs of idiomorphic chrome spinel grains from sample KAR1 (Lower Triassic Gerence Formation).

Fig. 11 Tectonic discrimination for samples from the Karaburun Peninsula and the islands of Chios and Inousses. (a) Diagram after Roser and Korsch (1986). PM – passive margin; ACM – active continental margin; ARC – oceanic island arc margin. (b) Multidimensional diagram after Verma and Armstrong-Altrin (2013) for discrimination of tectonic settings (63%<SiO_2<95%). Arc – island or continental arc; Rift – continental rift; Col – collision. (c, d) Multidimensional discriminant function diagrams for the discrimination of active and passive margin settings after Verma and Armstrong-Altrin (2016). See Figure 10 for explanation of symbols.

Fig. 12 Composition of garnets in the ternary classification scheme of Mange and

Morton (2007) with idealised almandine + spessartine (Alm+Sps), pyrope (Prp) and grossular (Grs) compositions as poles. Pie charts give percentage distribution of garnet types. Garnet types: A — sourced from granulite facies metasediments, charnockites or intermediate to felsic deeper crust rocks; Bi — from intermediate to felsic igneous rocks; Bii — from amphibolite-facies metasediments; Ci — from high-grade metamafic rocks; Cii — from ultramafic rocks with high Mg; D — from Ca-rich metamorphites like metasomatic rocks (skarns), very low-grade metabasic rocks or ultra-high temperature calc-silicate granulites.

Fig. 13 (a) Plot of Nb versus Cr contents of detrital rutiles with discrimination line from Triebold et al. (2012). (b) Percentage distribution of rutile derived from felsic and mafic rocks. (c) Histograms of calculated formation temperatures for metamafic and metapelitic rutiles.

Fig. 14 Compositional data for detrital chrome spinel from the Lower Triassic Gerence Formation and Upper Palaeozoic Alandere and Küçükbahçe formations. Grey symbols represent data from Upper Palaeozoic and Lower Mesozoic sediments of Chios (taken from Meinhold et al., 2007). Coloured fields refer to compositions of chrome spinel from the Dobromirtsi Ultramafic Massif in Bulgaria (González-Jiménez et al., 2015) and the Elekdağ ophiolite in northern Turkey (Dönmez et al., 2014). The age of the Dobromirtsi ophiolite is unknown – its protoliths have been considered to be Precambrian, Palaeozoic or Mesozoic. A Palaeozoic age is supported by a prominent Os model-age peak at 0.4 Ga from platinum-group minerals in chromite (González-Jiménez et al., 2015). (a) TiO_2 versus Al_2O_3 diagram with Cr-spinel discrimination fields (after Kamenetsky et al., 2001). LIP — large igneous province, OIB — ocean-island basalts, ARC — island-arc basalts; MORB — mid-ocean ridge basalts, SSZ — supra-subduction zone. (b) Cr- and Mg-numbers with discrimination fields for harzburgites and lherzolites (after Pober and Faupl, 1988). (c) TiO_2 versus Cr#

diagram for tectonic discrimination (after Pagé and Barnes, 2009).

Fig. 15 Crystallisation age minus depositional age versus cumulative proportion of detrital zircon ages (after Cawood et al., 2012). Data for samples from the Karaburun Peninsula are from Löwen et al. (2017) and for the islands of Chios and Inousses are from Meinhold et al. (2008) and Meinhold and Frei (2008), respectively.

Fig. 16 Compilation of information on tectonic settings based on petrographical, geochemical and geochronological data from the Karaburun Peninsula. (a) Diagrams after Dickinson et al. (1983). (b) Diagrams after Roser and Korsch (1986). (c) Diagrams after Verma and Armstrong-Altrin (2013). (d, e) Diagrams after Verma and Armstrong-Altrin (2016). (f) Determination of tectonic setting after Cawood et al. (2012).

Fig. 17 Palaeogeographic reconstruction indicating the supposed position of some of the Chios–Karaburun units in Carboniferous time (after Stampfli and Borel, 2002). CK: Chios–Karaburun units, Sk: Sakarya, Rh: Rhodope, Pl: Pelagonia, Mn: Menderes, Ta: Taurides.

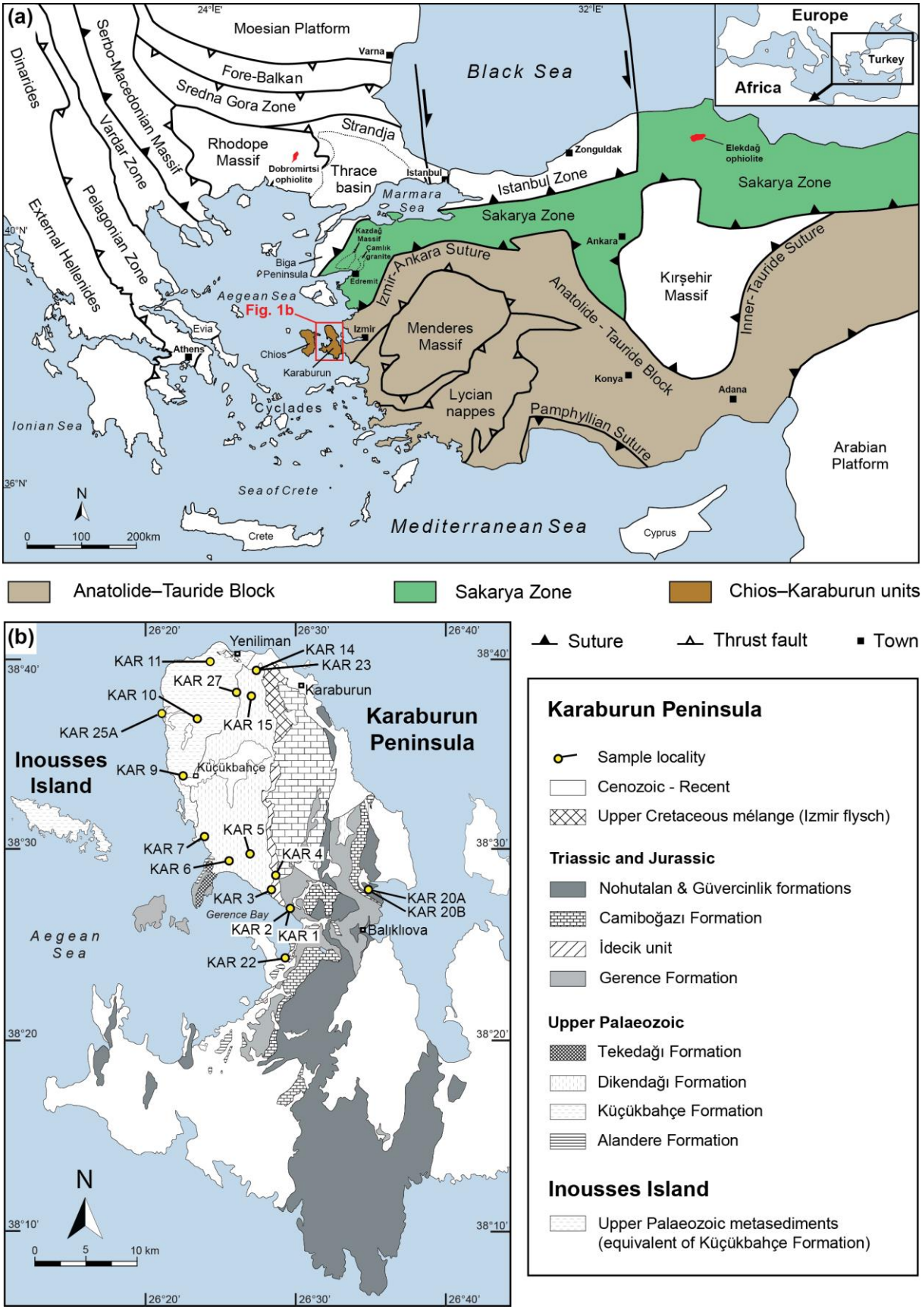
(a)
Moesian Platform
Black Sea
Europe
Africa
Turkey
Varna
Fore-Balkan
Sredna Gora Zone
Dinarides
Serbo-Macedonian Massif
Vardar Zone
Pelagonian Zone
External Hellenides
Rhodope Massif
Dobromirtsi ophiolite
Strandja
Thrace basin
Istanbul
Zonguldak
Elekdağ ophiolite
Istanbul Zone
Sakarya Zone
Marmara Sea
Kazdağ Massif
Çamlık granite
Biga Peninsula
Edremit
Izmir-Ankara Suture
Ankara
Kırşehir Massif
Inner-Tauride Suture
Aegean Sea
Fig. 1b
Evia
Athens
Izmir
Chios
Karaburun
Menderes Massif
Anatolide - Tauride Block
Konya
Adana
Cyclades
Lycian nappes
Pamphyllian Suture
Ionian Sea
Arabian Platform
Sea of Crete
Mediterranean Sea
Crete
Cyprus
Anatolide–Tauride Block
Sakarya Zone
Chios–Karaburun units
Suture
Thrust fault
Town
(b)
Yeniliman
KAR 11
KAR 14
KAR 23
KAR 27
Karaburun
KAR 10
KAR 15
KAR 25A
Karaburun Peninsula
Inousses Island
KAR 9
Küçükbahçe
KAR 5
KAR 7
KAR 4
KAR 6
KAR 3
KAR 20A
KAR 20B
Gerence Bay
KAR 2
KAR 1
Balıklıova
Aegean Sea
KAR 22
Karaburun Peninsula
Sample locality
Cenozoic - Recent
Upper Cretaceous mélange (Izmir flysch)
Triassic and Jurassic
Nohutalan & Güvercinlik formations
Camiboğazı Formation
İdecik unit
Gerence Formation
Upper Palaeozoic
Tekedağı Formation
Dikendağı Formation
Küçükbahçe Formation
Alandere Formation
Inousses Island
Upper Palaeozoic metasediments
(equivalent of Küçükbahçe Formation)

Fig. 1

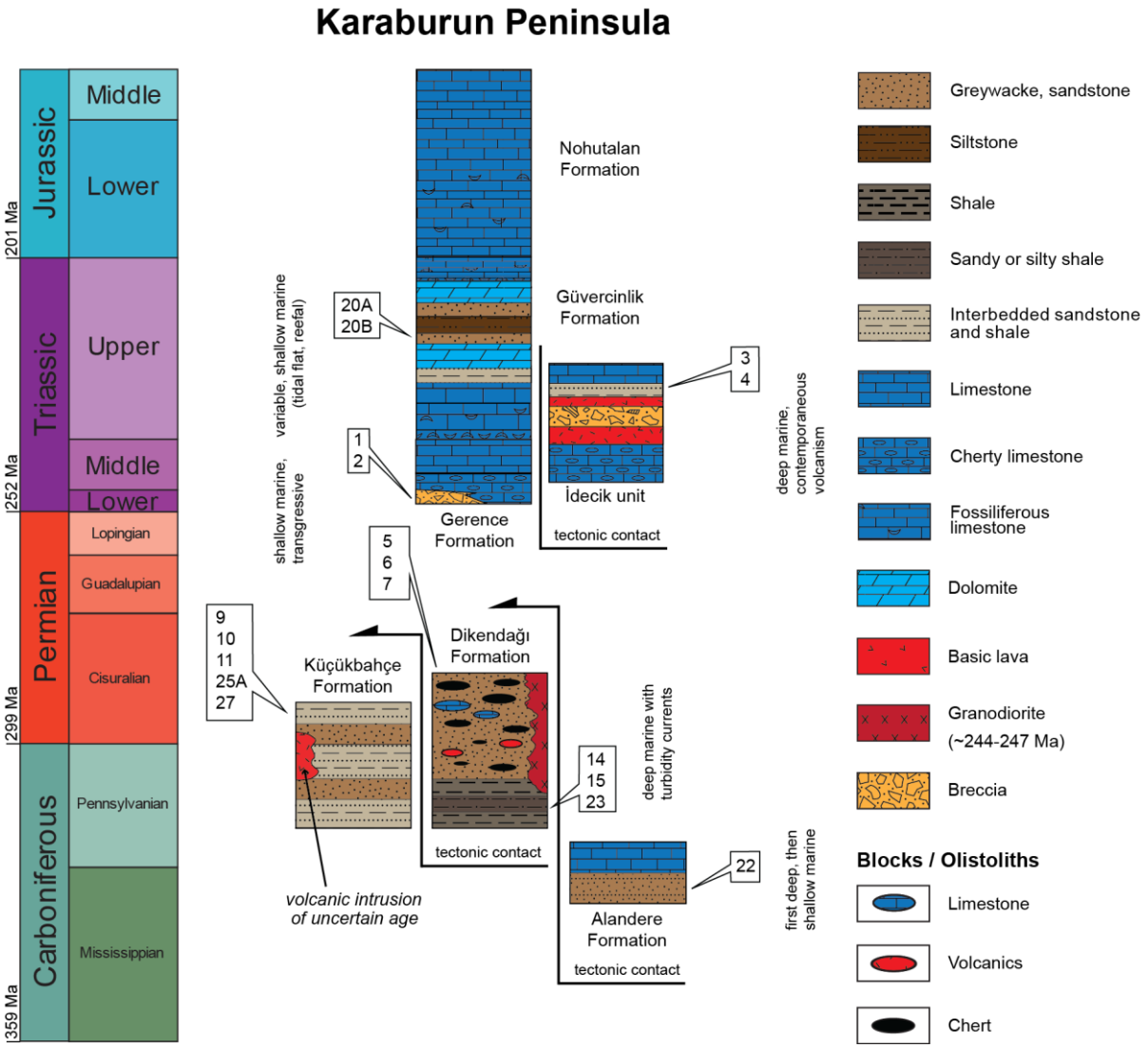
Karaburun Peninsula
Jurassic
Middle
Lower
Triassic
Upper
Middle
Lower
Permian
Lopingian
Guadalupian
Cisuralian
Carboniferous
Pennsylvanian
Mississippian
201 Ma
252 Ma
299 Ma
359 Ma
Nohutalan Formation
Güvercinlik Formation
İdecik unit
tectonic contact
Gerence Formation
Dikendağı Formation
Küçükbahçe Formation
tectonic contact
Alandere Formation
tectonic contact
volcanic intrusion of uncertain age
variable, shallow marine (tidal flat, reefal)
shallow marine, transgressive
deep marine, contemporaneous volcanism
deep marine with turbidity currents
first deep, then shallow marine
20A
20B
1
2
3
4
5
6
7
9
10
11
25A
27
14
15
23
22
Greywacke, sandstone
Siltstone
Shale
Sandy or silty shale
Interbedded sandstone and shale
Limestone
Cherty limestone
Fossiliferous limestone
Dolomite
Basic lava
Granodiorite (~244-247 Ma)
Breccia
Blocks / Olistoliths
Limestone
Volcanics
Chert

Fig. 2

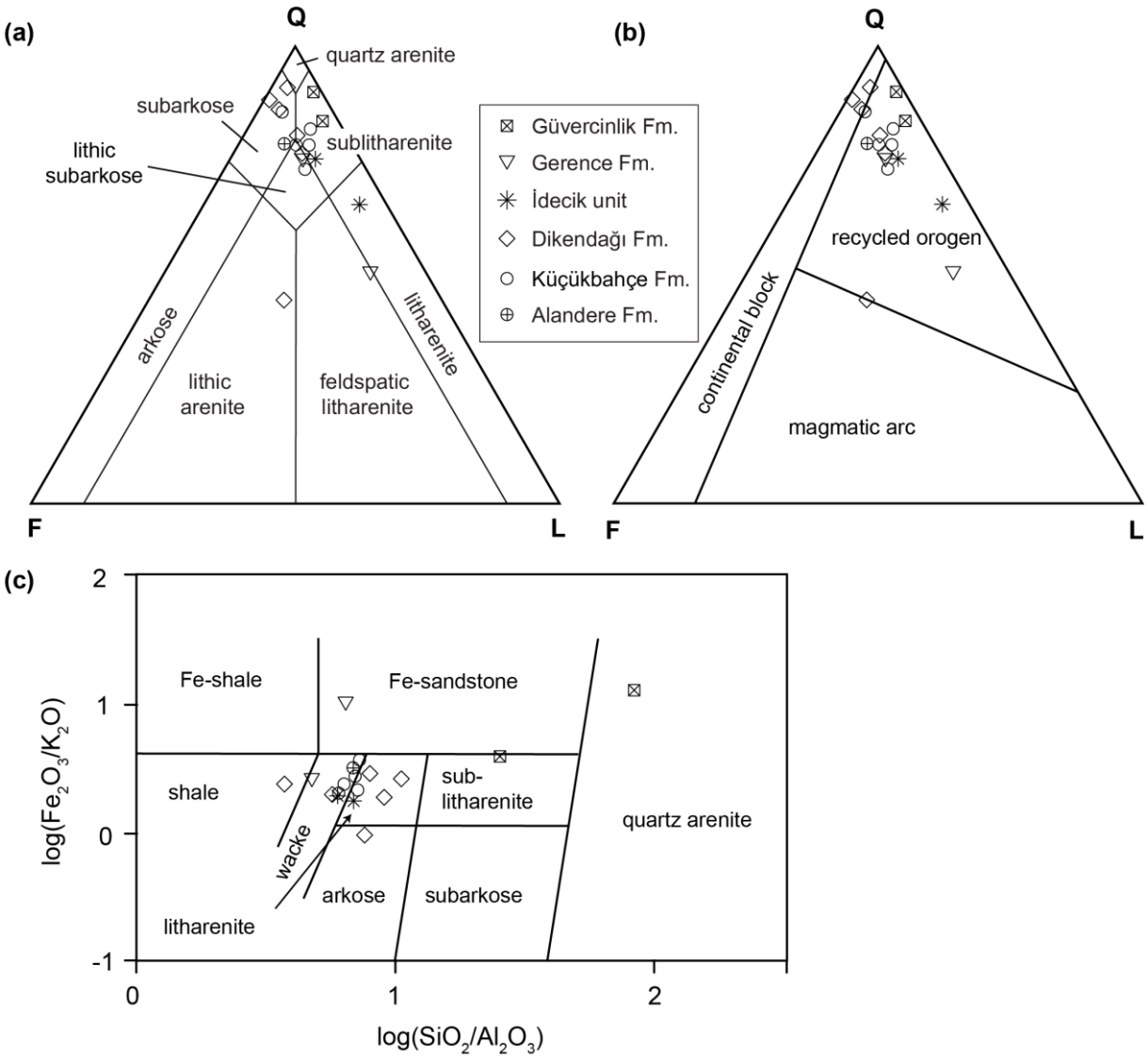
(a)
Q
quartz arenite
subarkose
lithic
subarkose
sublitharenite
arkose
litharenite
lithic
arenite
feldspatic
litharenite
F
L
Güvercinlik Fm.
Gerence Fm.
İdecik unit
Dikendağı Fm.
Küçükbahçe Fm.
Alandere Fm.
(b)
Q
recycled orogen
continental block
magmatic arc
F
L
(c)
Fe-shale
Fe-sandstone
shale
sub-
litharenite
quartz arenite
wacke
arkose
subarkose
litharenite
log(Fe2O3/K2O)
log(SiO2/Al2O3)
2
1
0
-1
0
1
2

Fig. 3

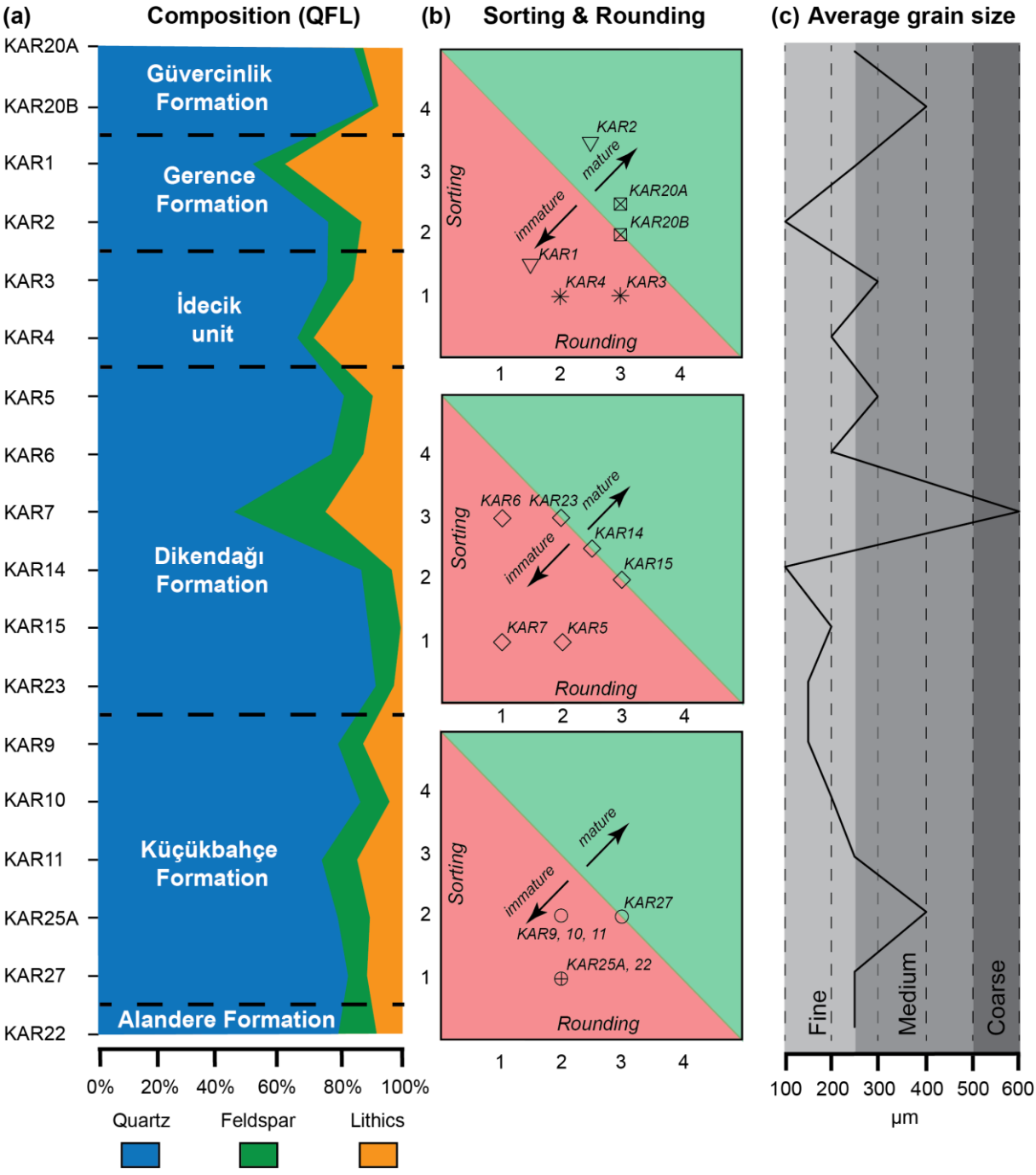
(a)
Composition (QFL)
(b)
Sorting & Rounding
(c) Average grain size
KAR20A
KAR20B
KAR1
KAR2
KAR3
KAR4
KAR5
KAR6
KAR7
KAR14
KAR15
KAR23
KAR9
KAR10
KAR11
KAR25A
KAR27
KAR22
Güvercinlik Formation
Gerence Formation
İdecik unit
Dikendağı Formation
Küçükbahçe Formation
Alandere Formation
0%
20%
40%
60%
80%
100%
Quartz
Feldspar
Lithics
Sorting
Rounding
mature
immature
KAR2
KAR20A
KAR20B
KAR1
KAR4
KAR3
KAR6
KAR23
KAR14
KAR15
KAR7
KAR5
KAR27
KAR9, 10, 11
KAR25A, 22
1
2
3
4
Fine
Medium
Coarse
100
200
300
400
500
600
µm

Fig. 4

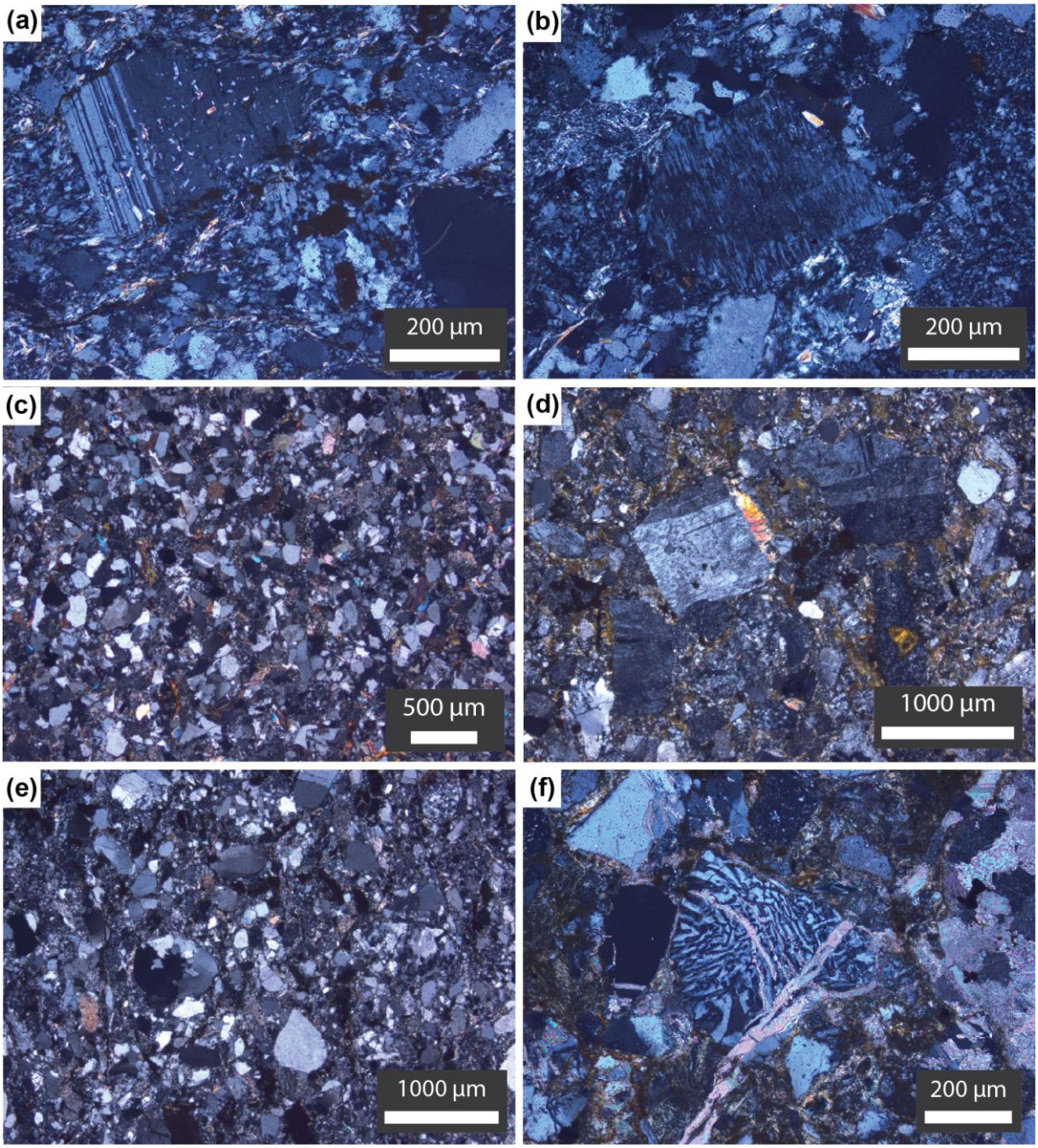

Fig. 5

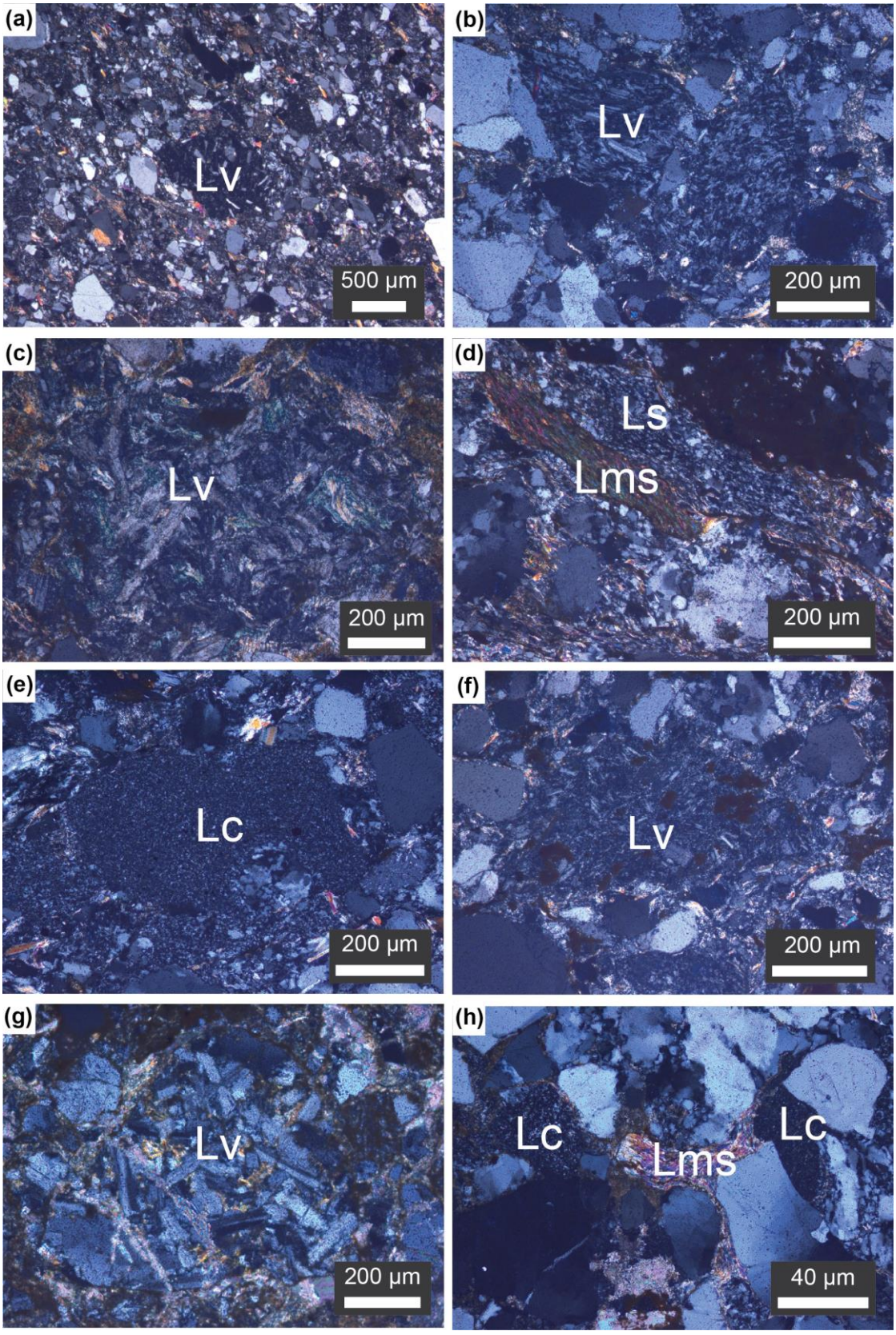
(a)
Lv
500 µm
(b)
Lv
200 µm
(c)
Lv
200 µm
(d)
Ls
Lms
200 µm
(e)
Lc
200 µm
(f)
Lv
200 µm
(g)
Lv
200 µm
(h)
Lc
Lms
Lc
40 µm

Fig. 6

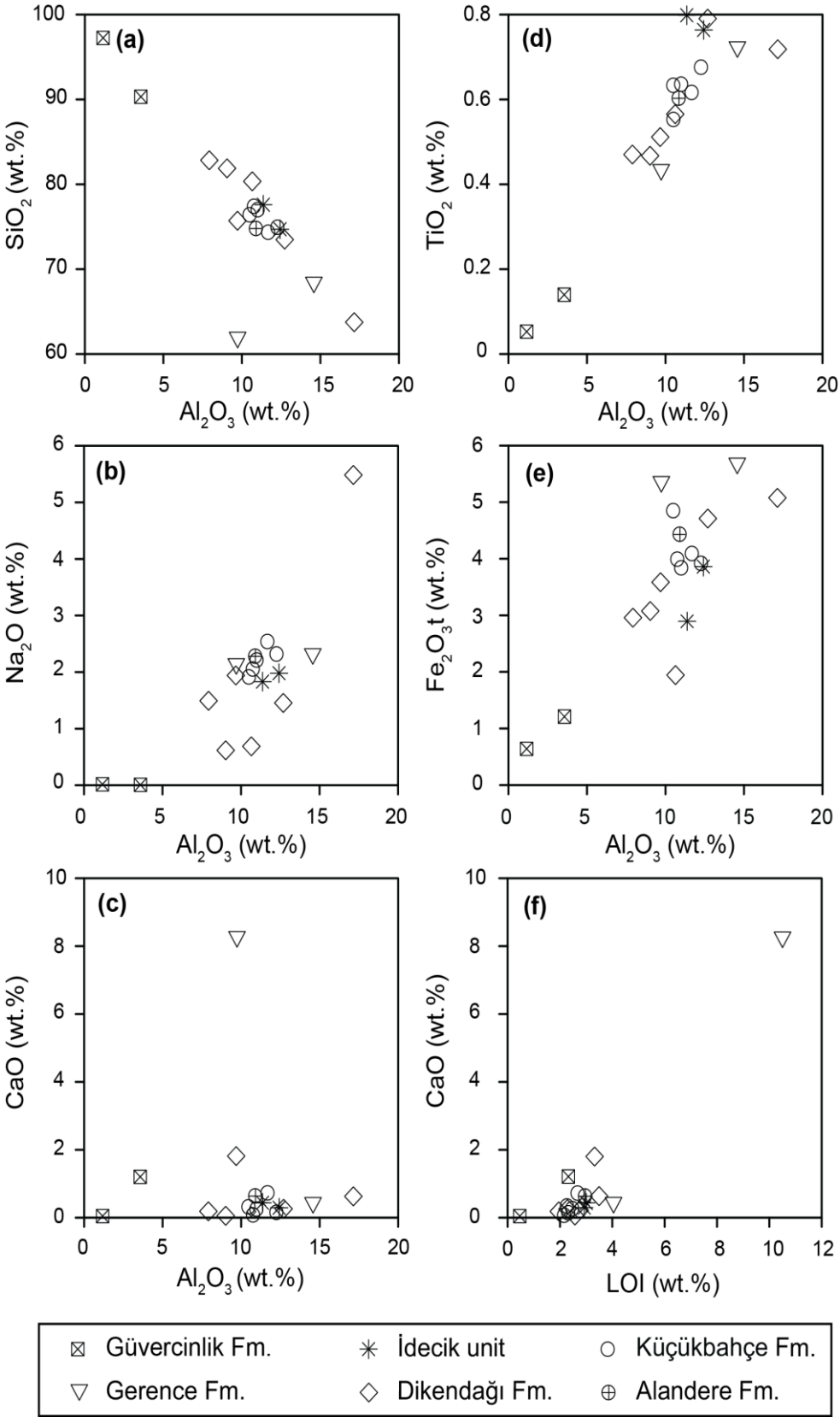
(a)
(b)
(c)
(d)
(e)
(f)
SiO2 (wt.%)
Na2O (wt.%)
CaO (wt.%)
TiO2 (wt.%)
Fe2O3t (wt.%)
CaO (wt.%)
Al2O3 (wt.%)
Al2O3 (wt.%)
Al2O3 (wt.%)
Al2O3 (wt.%)
Al2O3 (wt.%)
LOI (wt.%)
Güvercinlik Fm.
İdecik unit
Küçükbahçe Fm.
Gerence Fm.
Dikendağı Fm.
Alandere Fm.

Fig. 7

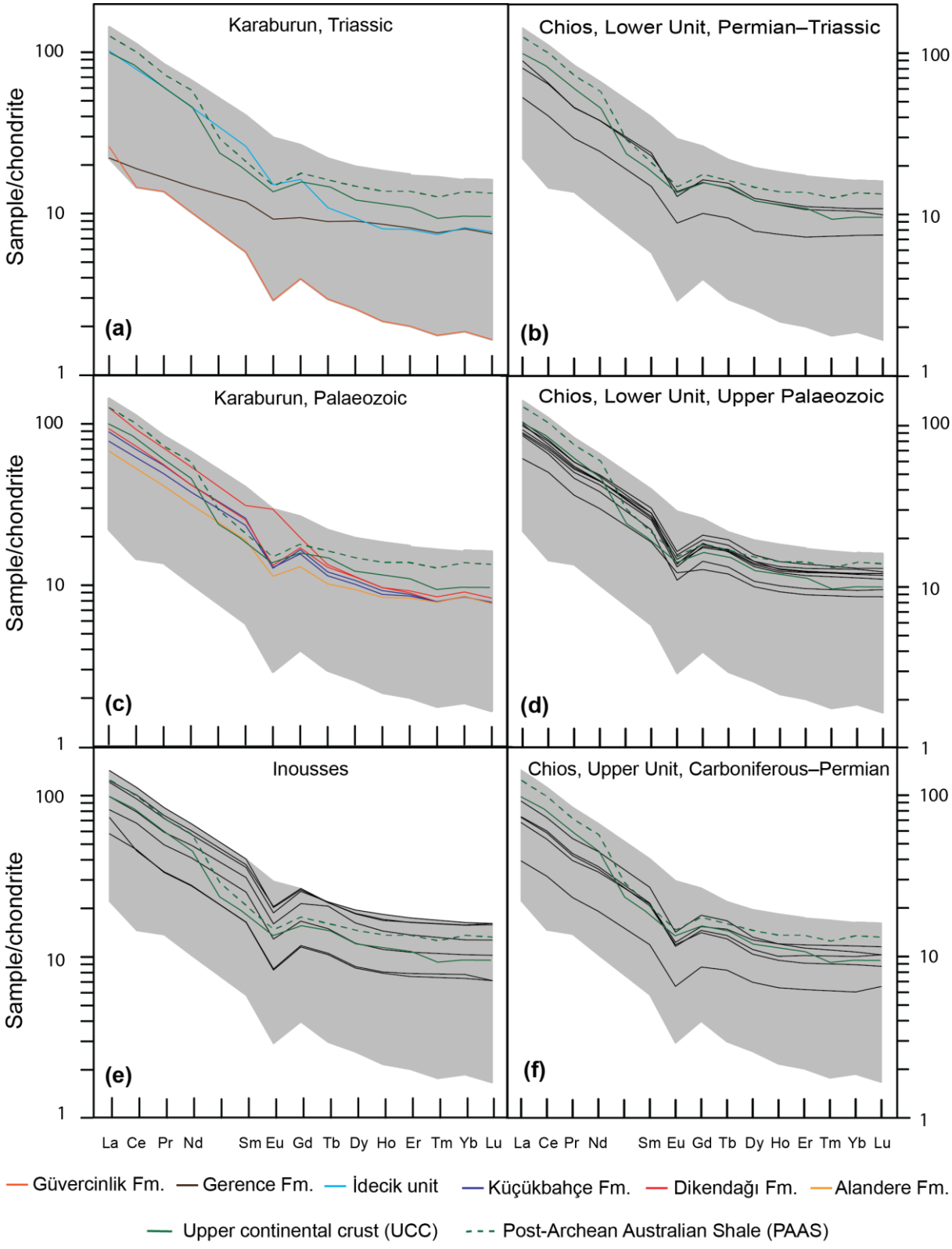
Karaburun, Triassic
Chios, Lower Unit, Permian–Triassic
Karaburun, Palaeozoic
Chios, Lower Unit, Upper Palaeozoic
Inousses
Chios, Upper Unit, Carboniferous–Permian
(a)
(b)
(c)
(d)
(e)
(f)
Sample/chondrite
100
10
1
La Ce Pr Nd Sm Eu Gd Tb Dy Ho Er Tm Yb Lu
Güvercinlik Fm.
Gerence Fm.
İdecik unit
Küçükbahçe Fm.
Dikendağı Fm.
Alandere Fm.
Upper continental crust (UCC)
Post-Archean Australian Shale (PAAS)

Fig. 8

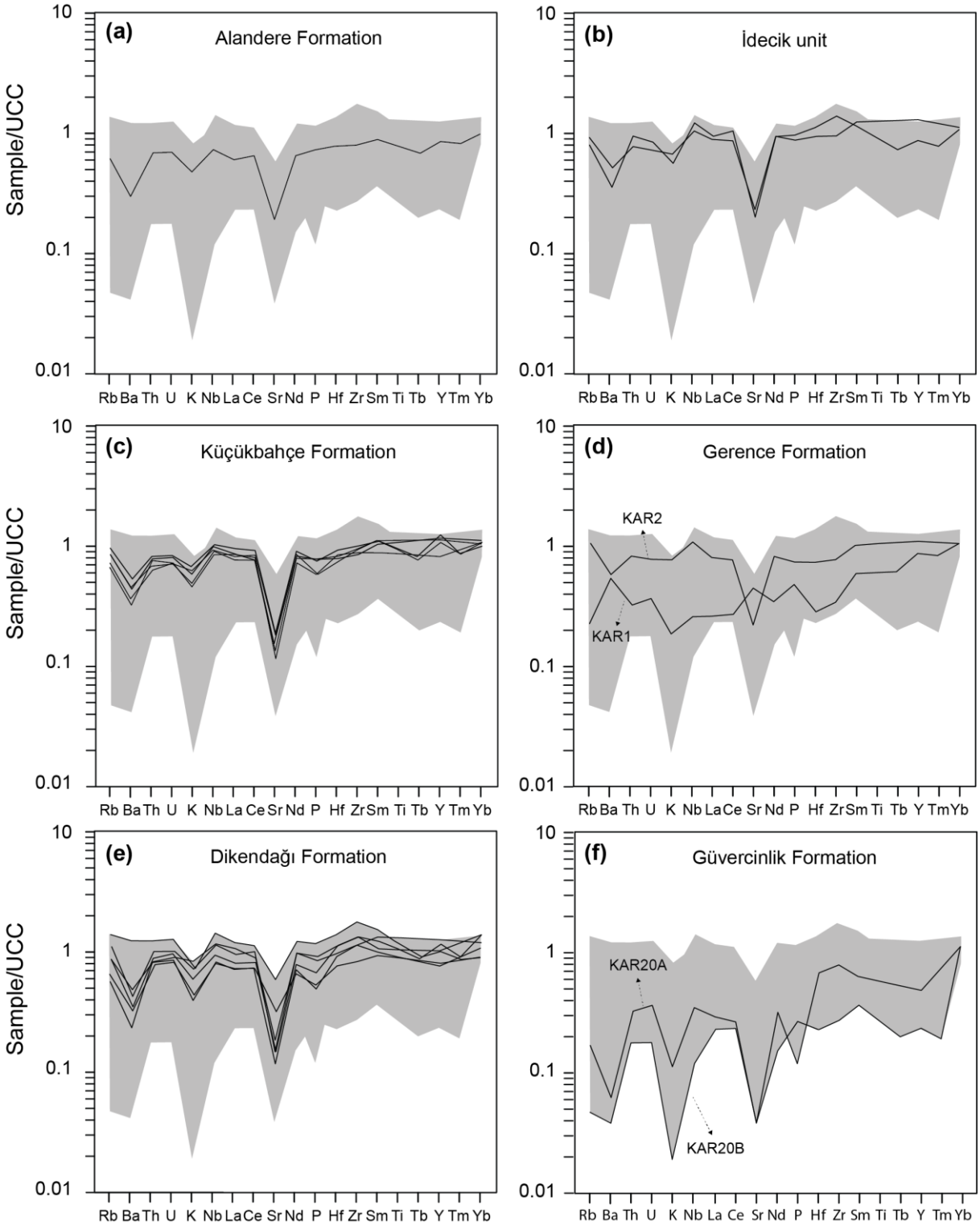
(a)
Alandere Formation
(b)
İdecik unit
(c)
Küçükbahçe Formation
(d)
Gerence Formation
KAR2
KAR1
(e)
Dikendağı Formation
(f)
Güvercinlik Formation
KAR20A
KAR20B
Sample/UCC
10
1
0.1
0.01
Rb Ba Th U K Nb La Ce Sr Nd P Hf Zr Sm Ti Tb Y Tm Yb

Fig. 9

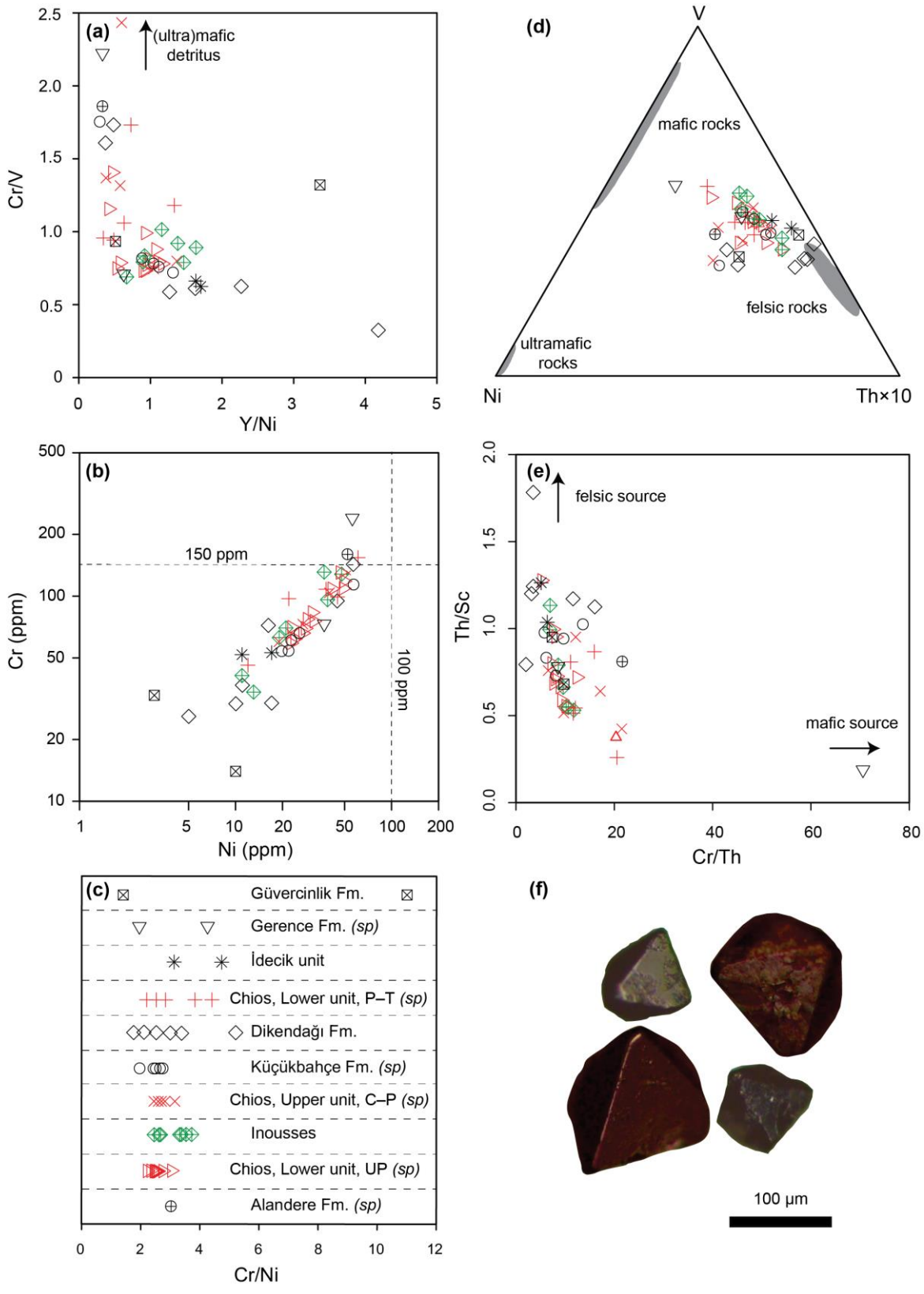
(a)
(ultra)mafic detritus
Cr/V
Y/Ni
(b)
150 ppm
100 ppm
Cr (ppm)
Ni (ppm)
(c)
Güvercinlik Fm.
Gerence Fm. (sp)
İdecik unit
Chios, Lower unit, P–T (sp)
Dikendağı Fm.
Küçükbahçe Fm. (sp)
Chios, Upper unit, C–P (sp)
Inousses
Chios, Lower unit, UP (sp)
Alandere Fm. (sp)
Cr/Ni
(d)
V
mafic rocks
felsic rocks
ultramafic rocks
Ni
Th×10
(e)
felsic source
mafic source
Th/Sc
Cr/Th
(f)
100 µm

Fig. 10

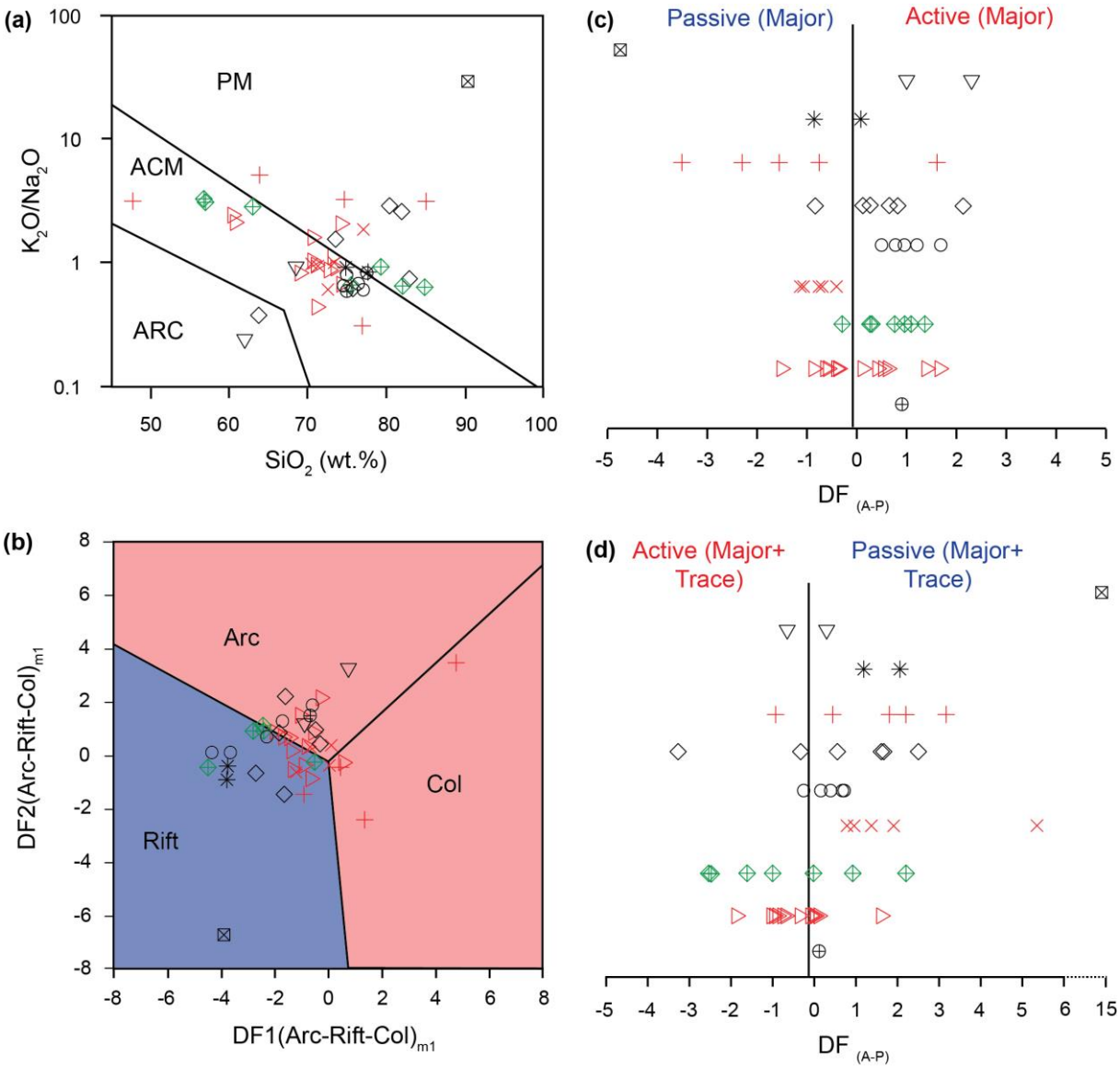
(a)
PM
ACM
ARC
K_2O/Na_2O
SiO_2 (wt.%)
(b)
Arc
Col
Rift
DF2(Arc-Rift-Col)$_{m1}$
DF1(Arc-Rift-Col)$_{m1}$
(c)
Passive (Major)
Active (Major)
DF $_{(A-P)}$
(d)
Active (Major+ Trace)
Passive (Major+ Trace)
DF $_{(A-P)}$

Fig. 11

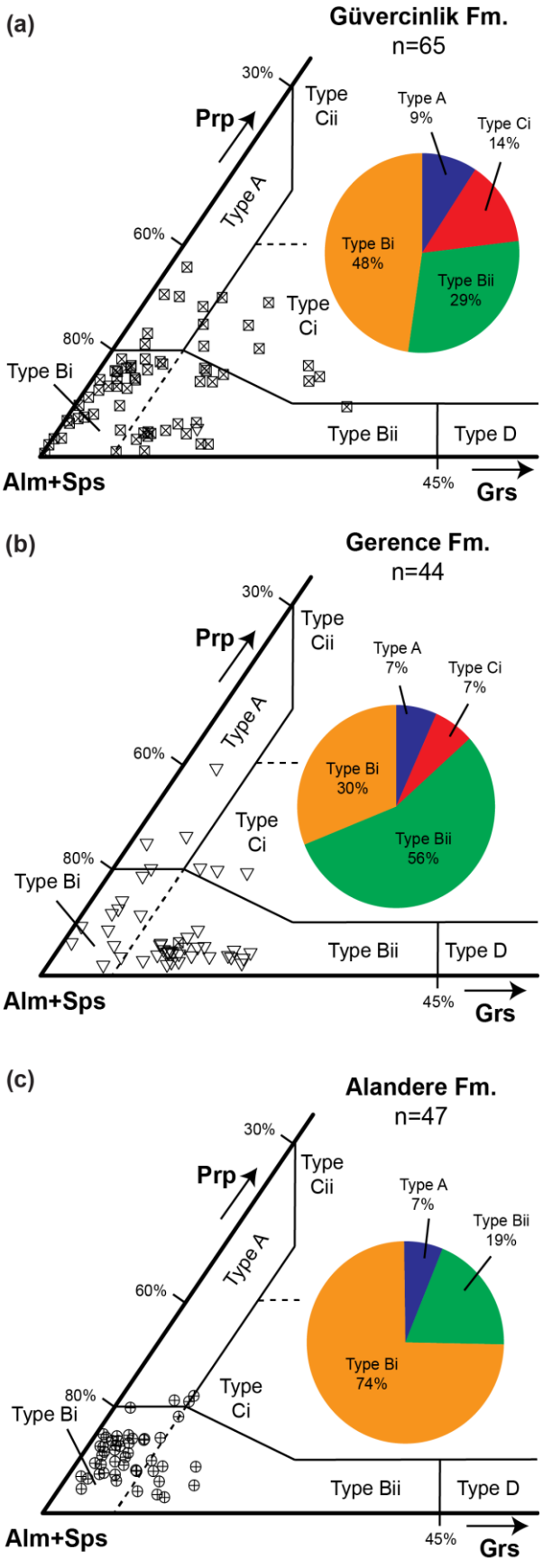
(a)
Güvercinlik Fm.
n=65
30%
Type Cii
Prp
Type A
60%
Type Ci
80%
Type Bi
Type Bii
Type D
Alm+Sps
45%
Grs
Type A 9%
Type Ci 14%
Type Bi 48%
Type Bii 29%
(b)
Gerence Fm.
n=44
30%
Type Cii
Prp
Type A
60%
Type Ci
80%
Type Bi
Type Bii
Type D
Alm+Sps
45%
Grs
Type A 7%
Type Ci 7%
Type Bi 30%
Type Bii 56%
(c)
Alandere Fm.
n=47
30%
Type Cii
Prp
Type A
60%
Type Ci
80%
Type Bi
Type Bii
Type D
Alm+Sps
45%
Grs
Type A 7%
Type Bii 19%
Type Bi 74%

Fig. 12

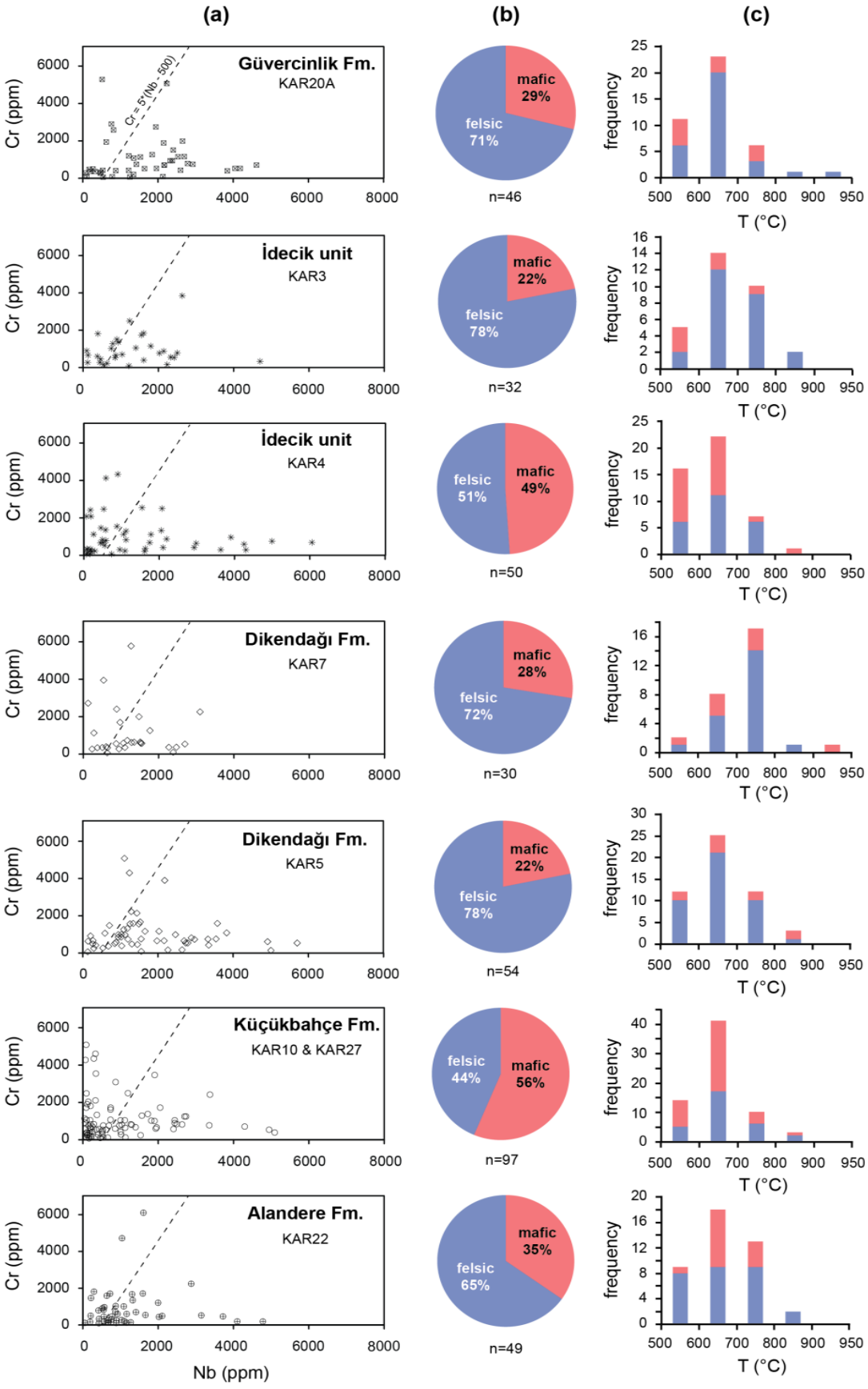
(a)
(b)
(c)
Güvercinlik Fm.
KAR20A
Cr = 5*(Nb - 500)
İdecik unit
KAR3
İdecik unit
KAR4
Dikendağı Fm.
KAR7
Dikendağı Fm.
KAR5
Küçükbahçe Fm.
KAR10 & KAR27
Alandere Fm.
KAR22
Cr (ppm)
Nb (ppm)
mafic 29%
felsic 71%
n=46
mafic 22%
felsic 78%
n=32
felsic 51%
mafic 49%
n=50
mafic 28%
felsic 72%
n=30
mafic 22%
felsic 78%
n=54
felsic 44%
mafic 56%
n=97
mafic 35%
felsic 65%
n=49
frequency
T (°C)

Fig. 13

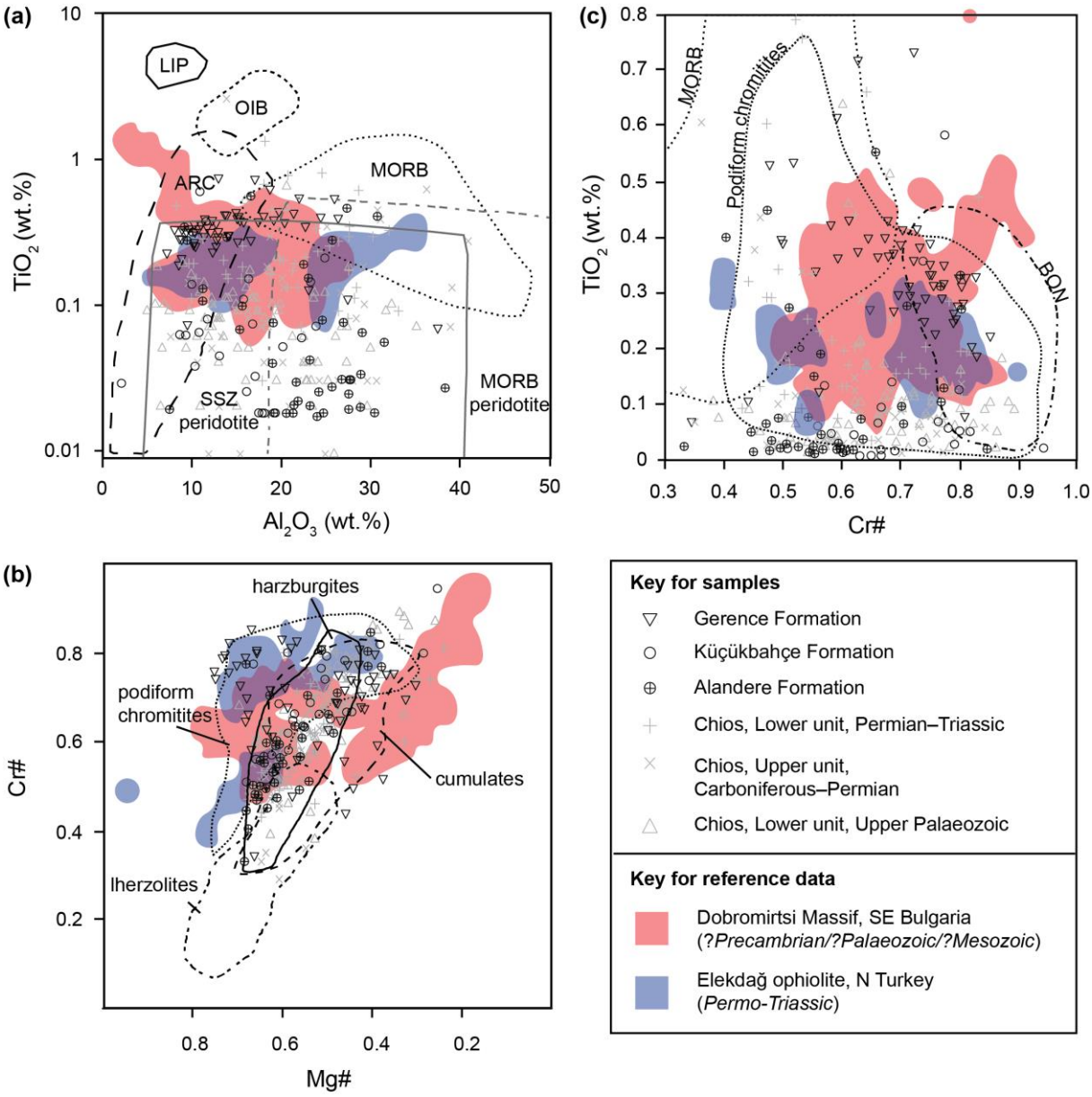
(a)
LIP
OIB
ARC
MORB
SSZ peridotite
MORB peridotite
TiO2 (wt.%)
Al2O3 (wt.%)
(c)
MORB
Podiform chromitites
BON
TiO2 (wt.%)
Cr#
(b)
harzburgites
podiform chromitites
cumulates
lherzolites
Cr#
Mg#
Key for samples
Gerence Formation
Küçükbahçe Formation
Alandere Formation
Chios, Lower unit, Permian–Triassic
Chios, Upper unit, Carboniferous–Permian
Chios, Lower unit, Upper Palaeozoic
Key for reference data
Dobromirtsi Massif, SE Bulgaria (?Precambrian/?Palaeozoic/?Mesozoic)
Elekdağ ophiolite, N Turkey (Permo-Triassic)

Fig. 14

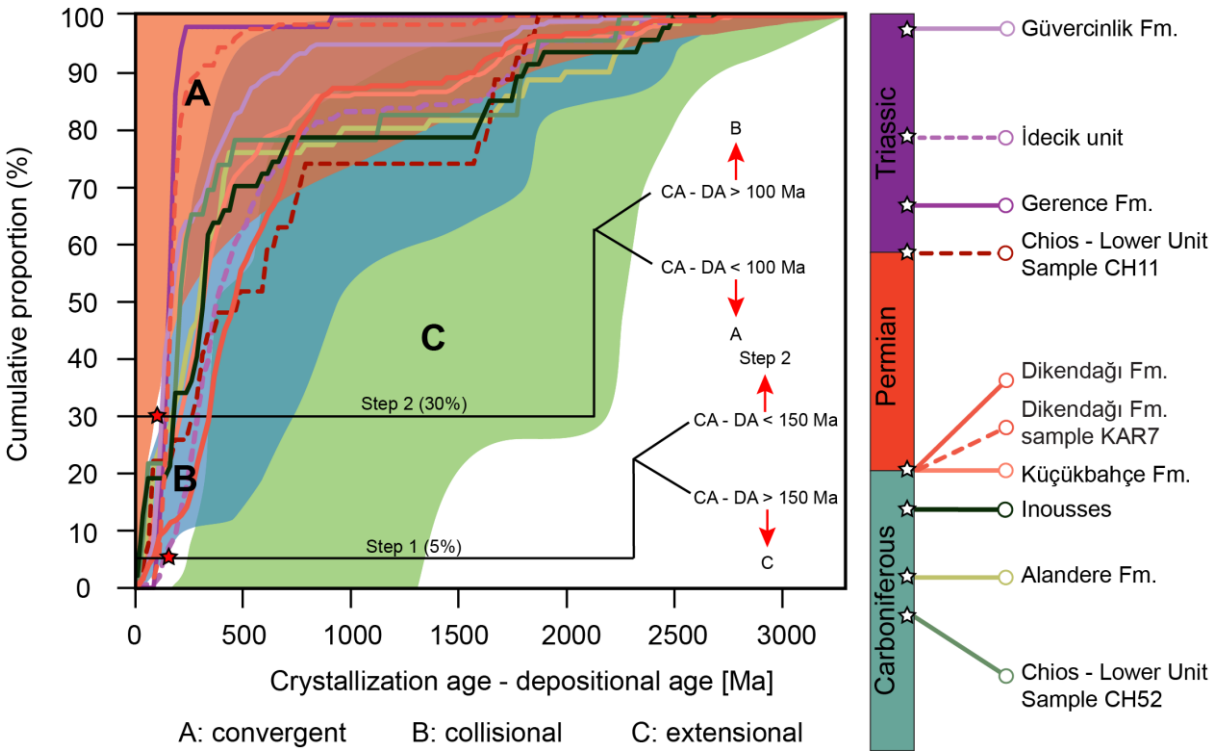
Cumulative proportion (%)
100
90
80
70
60
50
40
30
20
10
0
A
B
C
Step 2 (30%)
Step 1 (5%)
B
CA - DA > 100 Ma
CA - DA < 100 Ma
A
Step 2
CA - DA < 150 Ma
CA - DA > 150 Ma
C
0
500
1000
1500
2000
2500
3000
Crystallization age - depositional age [Ma]
A: convergent
B: collisional
C: extensional
Triassic
Permian
Carboniferous
Güvercinlik Fm.
İdecik unit
Gerence Fm.
Chios - Lower Unit
Sample CH11
Dikendağı Fm.
Dikendağı Fm.
sample KAR7
Küçükbahçe Fm.
Inousses
Alandere Fm.
Chios - Lower Unit
Sample CH52

Fig. 15

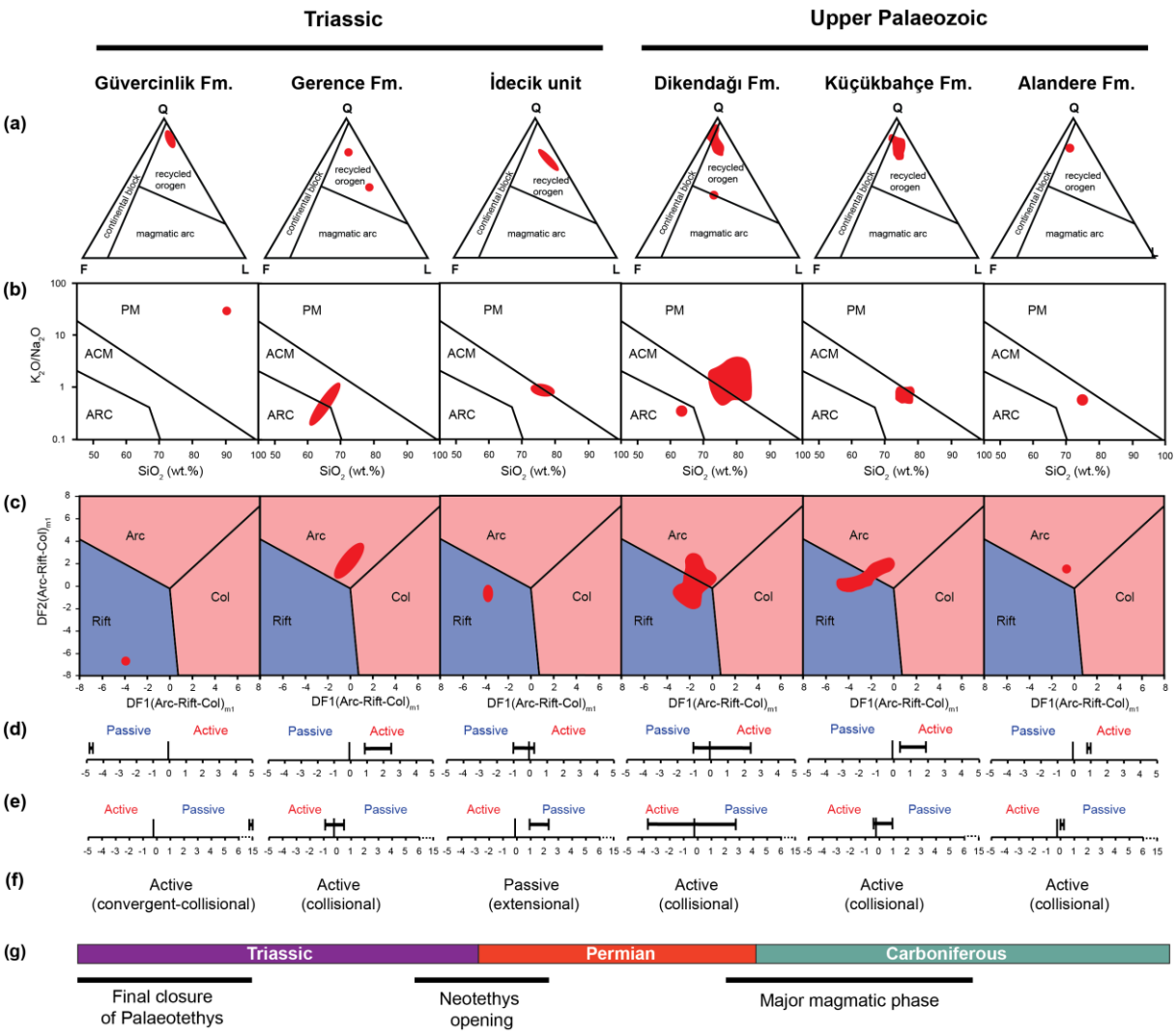
Triassic
Upper Palaeozoic
Güvercinlik Fm.
Gerence Fm.
İdecik unit
Dikendağı Fm.
Küçükbahçe Fm.
Alandere Fm.
(a)
Q
F
L
recycled orogen
continental block
magmatic arc
(b)
PM
ACM
ARC
K2O/Na2O
SiO2 (wt.%)
(c)
Arc
Col
Rift
DF2(Arc-Rift-Col)m1
DF1(Arc-Rift-Col)m1
(d)
Passive
Active
(e)
Active
Passive
(f)
Active (convergent-collisional)
Active (collisional)
Passive (extensional)
Active (collisional)
Active (collisional)
Active (collisional)
(g)
Triassic
Permian
Carboniferous
Final closure of Palaeotethys
Neotethys opening
Major magmatic phase

Fig. 16

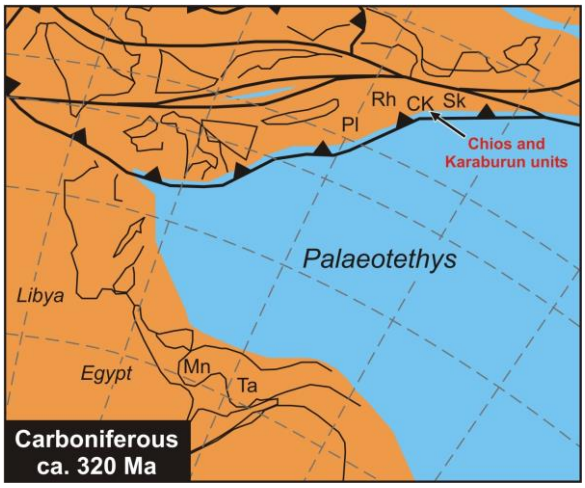
Rh
CK
Sk
Pl
Chios and
Karaburun units
Palaeotethys
Libya
Egypt
Mn
Ta
Carboniferous
ca. 320 Ma

Fig. 17

Table 1

Sample	Lithology	Geographic location	Geographic coordinates	QFL	XRF	ICP-MS	EMPA	U–Pb *
Güvercinlik Formation								
KAR20A	sublitharenite	N of Balıklıova	38°27'51.56"N, 26°35'23.41"E	X	X		X	X
KAR20B	sublitharenite	N of Balıklıova	38°27'51.56"N, 26°35'23.41"E	X	X	X		X
Gerence Formation								
KAR1	(feldspathic) litharenite	Gerence Bay	38°26'41.44"N, 26°30'08.24"E	X	X	X	X	X
KAR2	lithic subarkose	Gerence Bay	38°26'42.71"N, 26°30'50.86"E	X	X			
İdecik unit								
KAR3	sublitharenite	N of Gerence Bay	38°27'39.21"N, 26°28'37.59"E	X	X	X	X	X
KAR4	litharenite	N of Gerence Bay	38°28'24.21"N, 26°28'23.18"E	X	X		X	X
Dikendağı Formation								
KAR5	sublitharenite	N of Gerence Bay	38°29'39.03"N, 26°27'16.20"E	X	X		X	X
KAR6	lithic subarkose	N of Gerence Bay	38°29'14.58"N, 26°25'57.37"E	X	X			X
KAR7	lithic arenite	SW coast of Karaburun Peninsula	38°30'31.44"N, 26°24'17.82"E	X	X	X	X	X
KAR14	subarkose	SE of Yeniliman	38°39'25.02"N, 26°27'32.04"E	X	X	X		X
KAR15	subarkose	SSE of Yeniliman (close to granitoid intrusion)	38°38'00.70"N, 26°27'21.10"E	X	X			X
KAR23	subarkose	SE of Yeniliman						
Küçükbahçe Formation								
KAR9	sublitharenite	W of Küçükbahçe	38°33'48.12"N, 26°22'51.24"E	X	X	X		X
KAR10	subarkose	NW Karaburun Peninsula	38°36'44.64"N, 26°23'40.18"E	X	X		X	X
KAR11	lithic subarkose	W of Yeniliman	38°39'43.73"N, 26°24'27.59"E	X	X	X		X
KAR25A	lithic subarkose	NW coast of Karaburun Peninsula	38°37'05.10"N, 26°21'21.36"E	X	X			
KAR27	sublitharenite	S of Yeniliman; at contact to Dikendagi Formation	38°38'07.78"N, 26°26'34.40"E	X	X		X	X
Alandere Formation								
KAR22	subarkose	S of Gerence	38°24'05.34"N, 26°29'43.62"E	X	X	X	X	X

	Bay (coast)	

QFL – Petrographic thin-section analysis for conventional QFL classification; XRF – Major and trace element analysis using X-ray fluorescence spectrometry; ICP-MS – Rare earth element analysis using Inductively Coupled Plasma Mass Spectrometry; EMPA – Mineral chemical analysis using an electron microprobe analyzer; U–Pb – Detrital zircon U–Pb geochronology using laser ablation ICP-MS.
* Data from Löwen et al. (2017)

Table 2

Sample	Lithology	Qtz	Pl + Kfs	L	Bt	Ms	Chl	Cal	Grt	Cld	Ap	Ep	Tur	Zrn	Amp	Pyx	Rt	Ttn	Cr-Spl
Güvercinlik Formation																			
KAR 20A	sublithar enite	84	3	13	✚	✚	✚	⊙	⊙	–	–	–	⊙	⊙	⊙	⊙	⊙	⊙	–
KAR 20B	sublithar enite	91	1	8	–	–	✚	–	–	–	–	–	⊙	⊙	–	–	⊙	–	–
Gerence Formation																			
KAR 1	(feldspathic) litharenite	51	10	39	✚	✚	✚	✚	⊙	⊙	⊙	–	⊙	⊙	–	⊙	⊙	⊙	⊙
KAR 2	lithic subarkose	76	10	14	✚	✚	✚	–	–	⊙	–	–	–	⊙	⊙	–	⊙	–	–
İdecik unit																			
KAR 3	sublithar enite	76	8	16	–	✚	–	–	–	–	⊙	–	⊙	⊙	⊙	–	⊙	⊙	–
KAR 4	litharenite	66	5	29	–	✚	✚	⊙	–	⊙	–	–	⊙	⊙	⊙	–	–	–	–
Dikendağı Formation																			
KAR 5	sublithar enite	81	9	10	✚	✚	✚	–	–	–	⊙	⊙	⊙	⊙	⊙	–	⊙	⊙	–
KAR 6	subarkose	77	10	13	✚	✚	✚	⊙	–	–	–	–	–	⊙	–	–	–	⊙	–
KAR 7	lithic arenite	45	29	26	✚	✚	✚	⊙	–	–	–	–	⊙	⊙	–	–	⊙	⊙	–
KAR 14	subarkose	87	9*	4	✚	✚	–	–	–	–	⊙	–	⊙	⊙	–	–	⊙	⊙	–
KAR 15	subarkose	89	10	1	–	✚	✚	–	–	–	–	⊙	–	⊙	⊙	–	–	⊙	–
KAR 23	subarkose	92	5*	3	–	✚	–	–	–	–	–	⊙	⊙	⊙	–	–	⊙	⊙	–
Küçükbahçe Formation																			
KAR 9	sublithar enite	79	8	13	–	✚	–	–	–	⊙	–	–	⊙	⊙	–	–	⊙	–	–
KAR 10	subarkose	87	9	4	–	✚	✚	–	⊙	–	–	–	⊙	⊙	⊙	–	⊙	–	–
KAR 11	lithic arkose	74	11	15	–	✚	⊙	–	–	–	–	–	⊙	⊙	–	–	⊙	⊙	–

KA	lithic																		
R	subarkos	7		1	✚	✚	−	−	−	−	−	⊙	⊙	⊙	−	−	−	−	−
25A	e	9	10	1															
KA																			
R	sublithar	8		1	✚	✚	✚	⊙	−	−	−	−	⊙	⊙	−	−	⊙	⊙	⊙
27	enite	2	6	2															
Alandere Formation																			
KA																			
R	subarkos	7			✚	✚	✚	⊙	⊙	⊙	−	−	⊙	⊙	−	−	⊙	−	⊙
22	e	9	12	9															

✚ present; ⊙ accessory; − not observed; *no Kfs; Abbreviations: Qtz = quartz; Pl = plagioclase; Kfs = K-feldspar; L = lithic fragments; Bt = biotite; Ms = muscovite; Chl = chlorite;
Cal = calcite; Grt = garnet; Cld = chloritoid; Ap = apatite; Ep = epidote; Tur = tourmaline; Zrn = zircon; Amp = amphibole; Pyx = pyroxene; Rt = rutile; Ttn = titanite; Cr-Spl = Cr-Spinel

Table 3. Main observations from petrography, geochemistry and composition of heavy minerals

	Lithic fragments	Bulk-rock geochemistry	Single-grain geochemistry
Güvercinlik Formation	Rare; mainly (meta)sedimentary (Fig. 6h)	REE and trace element depletion relative to UCC (Figs. 8a, 9f)	Diverse garnet population; dominant input from intermediate to acidic igneous rocks and amphibolite-facies metasediments; rutiles were mainly derived from amphibolite- to eclogite-facies rocks
Gerence Formation	Abundant; primarily volcanic (Fig. 6g)	Indicative for (ultra)mafic material (Fig. 10) *KAR1*: HFSE depletion (Fig. 9d);	High amount of garnets derived from amphibolite-facies metasediments (~60%) and intermediate to felsic igneous rocks (~30%); chrome spinels with high Cr- and Mg-numbers are indicative of spinels from podiform chromitites
İdecik unit	Abundant; volcanic and meta-sedimentary (Fig. 6f)	Indicative of felsic rather than mafic sources (Fig. 10)	Variable rutile composition suggests mainly felsic source rocks; geothermometry data indicate amphibolite- to eclogite-facies source rocks; considerable amount of higher temperature (>700°C) rutiles (*KAR3*)
Dikendağı Formation	Rare; mainly (meta)sedimentary minor volcanic (Fig. 6b) *KAR7*: abundant volcanic fragments (Figs. 4, 6c)	Heterogeneous; Indicative of predominant felsic sources (Fig. 10)	Rutile compositional data indicate mainly metapelitic sources; geothermometry data reveal variable formation temperatures mainly between 600–700°C (*KAR5*) and 700–800°C (*KAR7*)
Küçükbahçe Formation	Low to moderate amount; mainly (meta)sedimentary (Fig. 6d, e) *KAR27:* abundant volcanic fragments	Homogeneous; dominant felsic sources; variable contribution from (ultra)mafic rocks (Fig. 10)	Rutile data reveal a mixed but dominant metamafic source of amphibolite- to eclogite-facies rocks; compositional data of chrome spinel show SSZ to MORB peridotite affinity and suggest a mixed source of dominant harzburgite and minor lherzolite composition
Alandere Formation	Rare; primarily volcanic (Fig. 6a)	Indicative of (ultra)mafic detritus (Fig. 10)	Homogeneous garnet compositions suggest mainly intermediate to felsic igneous source rocks; rutiles were derived from dominant felsic sources (~65%) of amphibolite- to granulite-facies rocks; chrome spinel compositions reveal MORB peridotite affinity and suggest a mixed source of dominant harzburgite and minor lherzolite composition

Highlights

- Provenance analysis of Palaeotethys-related sediments in western Turkey
- Sediment supply from terranes of the Balkans, the Sakarya Zone and/or equivalent units
- Deposition of Upper Palaeozoic sediments along the southern active margin of Eurasia
- Cr-spinels from the Triassic are indicative of detritus of podiform chromitites formed in an intra-oceanic back-arc setting